HYDRAULIC JUMPS AND STEPS: THE RELATIONSHIP BETWEEN JUMP LOCATION AND SEQUENT DEPTH RATIO USING A STEP

Nicholas Thomas Stephen Fowler

A research report submitted to the Faculty of Engineering and the Built Environment, University of the Witwatersrand, Johannesburg, in partial fulfilment of the requirements for the degree of Master of Science in Engineering.

Johannesburg, 2020

Declaration

I declare that this research report is my own unaided work. It is being submitted to the Degree of Master of Science to the University of the Witwatersrand, Johannesburg. It has not been submitted before for any degree or examination to any other University.

....

..........12th........ day of ....August................ year ....2020...........

Abstract

Abrupt steps used in stilling basins to dissipate energy are simple and effective structures, yet certain design aspects have been neglected. A series of small-scale laboratory experiments were conducted to investigate the effect of the position of the hydraulic jump and the effect of hysteresis on step design. Five new relationships were developed for relating the jump location to the step height and the upstream and downstream flow conditions. The findings show that the position of the jump influences the design, in addition to the significant benefit of physically quantifying the position of the jump. Furthermore, a sweep-out limitation was developed from the abrupt step testing, which has potential design implications. Lastly, the hysteresis effect on both abrupt and sloping steps was expanded, providing introductory influences on the sequent depths of the hydraulic jump and the position of the jump. The study provides introductory knowledge to the significance of the position of the hydraulic jump in the design, while expanding on established hysteric knowledge for steps.

Keywords: abrupt step, sloping step, hydraulic jump position/location, energy dissipation, stilling basin design, sweep-out, hysteresis

Acknowledgements

First and foremost, I would like to thank my supervisor Professor James whose guidance has made it possible to complete this research report. I have learnt a great deal of patience and persistence through your advice and analytical outlook. I would also like to thank Professor Taigbenu for his constant support throughout this process.

I would like to thank the laboratory staff of the school of Civil and Environmental Engineering who played a major role in this research project.

A special thanks to my girlfriend, Jade Crocket, for her unwavering support and patience.

Lastly, I must thank my parents for all the support and assistance that I have received throughout my studies. Without them, this would not be possible.

Table of contents

List of figures

List of tables

List of symbols

A	Cross-sectional area of flow
A_1	Cross-sectional area of flow in section 1
A_3	Cross-sectional area of flow in section 3
C	y-axis intercepts
E	Specific energy
E_1	Specific energy at section 1
E_2	Specific energy at section 2
E_3^*	Specific energy of the sequent flow downstream at section 2
E_3	Specific energy at section 3
E_3^*	Specific energy of the sequent flow downstream at section 3
E_{loss}	Energy loss over the step due to the step
E_c	Critical flow specific energy
F	Force on an object
F_{corr}	Force correction
$F_{hydrostatic}$	Hydrostatic force on the step
F_r	Froude number
F_{r1}	Upstream Froude number at section 1
F_{r3}	Downstream Froude number at section 3
g	Gravitational acceleration
h	Step height
h_{min}	Minimum step height before sweep-out
h_s	Vertical sill height
L_r	Roller length of a hydraulic jump induced by a step
L_r^*	Roller length of a simple hydraulic jump
M	Momentum function
M_1	Momentum function of upstream flow at section 1
M_2	Momentum function near the step at section 2
M_2^*	Momentum function of sequent flow near the step at section 2
M_3	Momentum function of downstream flow at section 3
M_3^*	Momentum function of sequent flow downstream at section 3

m	Gradients of linear equations for relationship 5 (Equation (4-20))
P	Force on the step
$P_{subcritical}$	Force on the step when subcritical flow occurs over the step
$P_{supercritical}$	Force on the step when supercritical flow occurs over the step
Q	Discharge of the flow
q	Unit discharge of the flow
V	Flow velocity
V_1	Flow velocity upstream at section 1
V_2	Flow velocity near the step at section 2
V_3	Flow velocity downstream at section 3
X	Distance between the toe of the hydraulic jump and the abrupt step
X_s	Hydraulic jump distance between toe and vertical sill
Y	Sequent depth ratio due to the sill or step $\left(\frac{y_3}{y_1}\right)$
Y^*	Sequent depth ratio of a simple hydraulic jump
y	Flow depth
y_1	Flow depth upstream at section 1
y_2	Flow depth near the step at section 2
y_2^*	Sequent flow depth near the step at section 2
y_3	Flow depth downstream at section 1
y_3^*	Sequent flow depth near the step at section 3
y_{3min}	Minimum flow depth at section 3 before sweep-out
Y_{corr}	$\frac{Y}{Y^*}$
Y_{diff}	$Y^* - Y$
ΔE	Energy losses due to the step height and energy dissipation
ΔY_f	Sequent depth ratio adjustment due to friction
ΔY_s	Sequent depth ratio adjustment due to the vertical sill
γ	Unit weight of water

1. Introduction

1.1. Prologue

The purpose of a stilling basin is to dissipate energy and change fast, supercritical flow into slow, subcritical flow within a section. The section or basin is often located at the exit of a water storage structure, such as a dam or reservoir. The exit can be a spillway or some other outlet structure, for example a sluice gate. The flow is released, via the exit of a storage facility, with high kinetic energy that needs to be dissipated to avoid erosion of the natural river channel (James, 2018). For the flow to dissipate its energy from supercritical to subcritical, the formation of a hydraulic jump is often the most effective method.

A hydraulic jump occurs in the channel when the flow is released without the aid of a structure to force the jump. This requires the slope of the channel to be mild and the supercritical flow to have a gradually varied profile, until the sequent depth of the downstream subcritical flow occurs. A hydraulic jump then occurs, changing the flow from supercritical to subcritical, as shown in Fig. 1-1. This is not practical as the jump will be far downstream of the outlet, causing a greater reach of the channel to be susceptible to erosion.

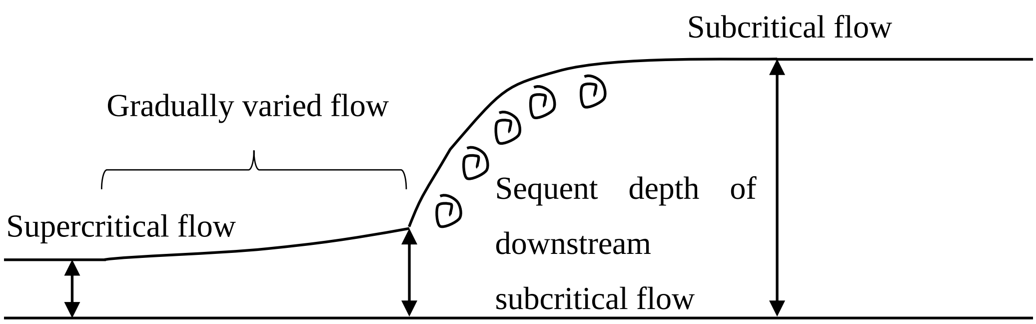

Figure 1-1- Formation of a hydraulic jump on a mild slope unassisted by a structure

It is therefore desirable to be able to control the hydraulic jump by forcing it to occur at a specific location or within a certain area. There are numerous ways this can be carried out and there is extensive research on energy dissipating structures for the purpose of stilling basin design. Common ones include, but are not limited to, sills, steps (upward and downward), and baffles. The United States Bureau of Reclamation (USBR) (Peterka, 1983) have created standard designs for stilling basins that can be applied to a wide range of conditions (James, 2018). However, a simple design is sometimes all that is required to induce a hydraulic jump and adequately dissipate the energy in the flow leaving the storage facility.

1.2. Aims of the investigation

An abrupt bottom channel rise or abrupt step is classified as a simple design that can be used in a stilling basin. This study aims to:

- expand the knowledge for abrupt step design in stilling basins by adapting and improving design relationships to ensure the formation and stability of a jump in the basin.
- develop a relationship or relationships that provide the correct sizing of the step and the exact location of the jump in the basin using the necessary flow conditions.

The concept of hysteresis is also explored as it could play a vital role in the design of stilling basins using steps. This study also aims to investigate the effect of hysteresis in the design of a stilling basin utilising both abrupt and sloping steps.

2. Literature review

2.1. Introduction

Countless research has been carried out regarding energy dissipation and energy dissipating structures in open channel hydraulics. With the focus on stilling basins, there is an abundance of research on energy dissipating structures, both simple and complex in their designs. Attention is concentrated on using an abrupt bottom channel rise or abrupt step incorporated in the design of a stilling basin.

The key design elements when utilising an abrupt step to dissipate energy in a stilling basin are the step height (*h*), the sequent depths of the hydraulic jump (y_1 and y_3), and the location of the hydraulic jump in the basin (*X*) depicted in Fig. 2-1. Most of the research carried out on abrupt step design focuses on the step height and the sequent depths that will ensure a hydraulic jump occurs in the stilling basin. Emphasis is placed on the stability of the hydraulic jump to ensure that it will not sweep-out of the basin or submerge the basin. However, little work has been done on quantifying the actual position of the jump in the basin.

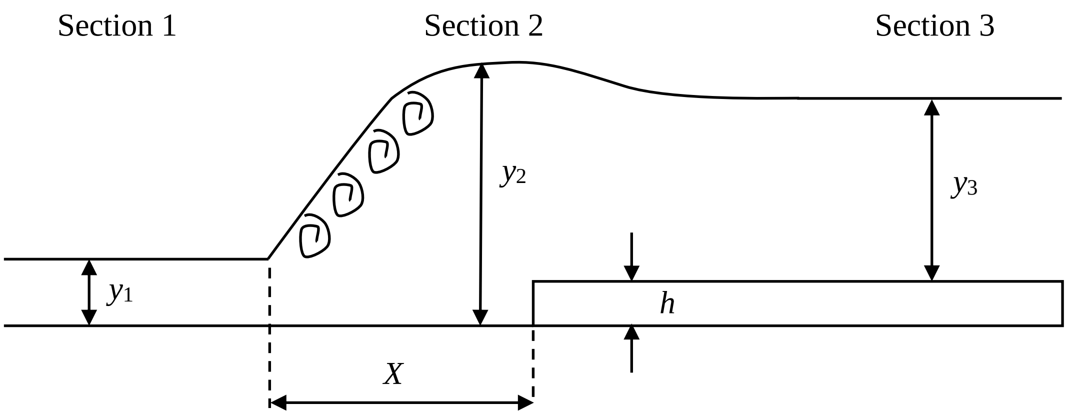

Figure 2-1- Hydraulic jump forced by a step and the associated design variables

The following review examines the developments of stilling basin design using an abrupt step, concentrating on the key elements required in the design. It then further focuses on the location of the hydraulic jump in the stilling basin and explores indirectly related research that has the potential to be applied to an abrupt step design. The review then looks at the effect of hysteresis on the design of steps in stilling basins.

2.2. Bottom channel rise or abrupt step

A bottom channel rise or abrupt step can be created by 'dropping' or excavating a section of the channel, at the exit of a spillway, to below the existing channel level (Fig. 2-2) or building a false bottom on top of the existing channel (Fig. 2-3). Several key factors in the design of abrupt steps are researched and discussed. These concepts will be reviewed individually and/or as a collective if they are interrelated.

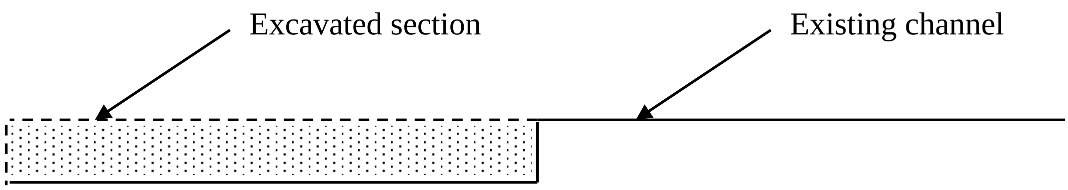

Figure 2-2- Excavated channel section to form the abrupt step

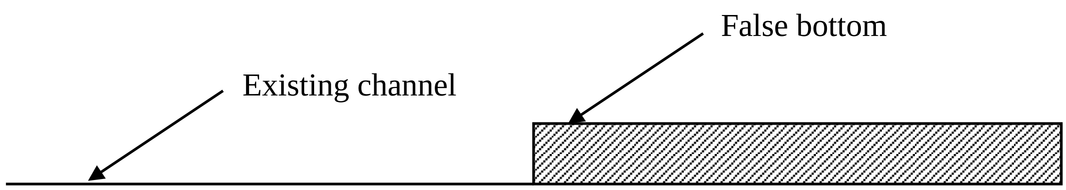

Figure 2-3- False bottom on top of the existing channel to form the abrupt step

2.2.1. Momentum and continuity

Multiple studies have examined the use of an abrupt step to induce a hydraulic jump (Forster and Skrinde (1950), Hager and Sinniger (1985), and Hager and Bretz (1986)). Most of them focused on ensuring the formation of a hydraulic jump in the basin and its stability, while less emphasis was placed on certain characteristics of the jump, such as its length and actual position.

The basic formulation of the relationships developed stemmed from the use of the force-momentum flux equation or momentum function equation for unit width in a horizontal, rectangular channel, and the continuity equation. The assumptions required in developing the equation to ensure the formation of a simple hydraulic jump are:

- boundary shear through the jump is negligible
- hydrostatic pressure distribution occurs before and after the jump
- uniform velocity distribution occurs before and after the jump
- that only external forces are acting on the free body

In order to develop the basic equation for a simple hydraulic jump, a solid object needs to be placed in the channel. The object is located between the supercritical and subcritical flows (Fig. 2-4).

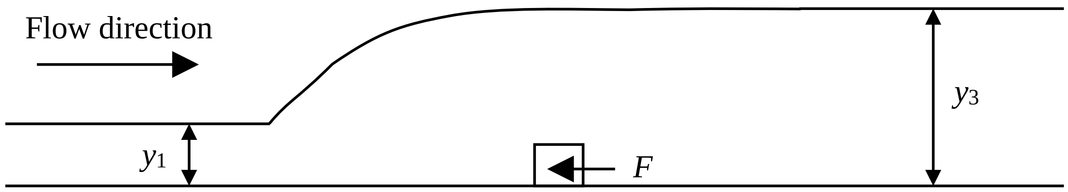

Figure 2-4- Object introduced into the channel for a simple hydraulic jump formulation

The difference in the momentums of the flows is equal to the force acting on the object (F):

$$\frac{F}{\gamma} = M_1 - M_3 \qquad (2\text{-}1)$$

where

F = The force acting the object (N/m)

γ = Unit weight of water (9810 kg $m^{-2}s^{-2}$)

$M_{1,3}$ = Momentum function (m^2/m)

The momentum functions ($M_{1,3}$), for rectangular channels of unit width, can be expressed as:

$$M = \frac{q^2}{gy} + \frac{y^2}{2} \tag{2-2}$$

where

y = Flow depth (m)

q = Unit discharge ($m^3/s/m$)

g = Gravitational acceleration (9.81 m/s^2)

For a simple hydraulic jump, there is no object in the channel, therefore F = 0. Furthermore, using the continuity equation:

$$Q = V_1 A_1 = V_3 A_3 \tag{2-3}$$

where

Q = Discharge (m^3/s)

$A_{1,3}$ = Cross-sectional area (m^2)

$V_{1,3}$ = Flow velocity (m/s)

and that the unit-width discharge $q = Vy$, the following equation was developed:

$$\frac{y_3}{y_1} = \frac{1}{2}\left(\sqrt{1 + 8{F_{r1}}^2} - 1\right) \tag{2-4}$$

Equation (2-4) presents a dimensionless relationship used to determine the sequent depth of a simple hydraulic jump with the use of the incoming flow's Froude number. The Froude number (F_{r1}) is the ratio of inertial and gravitational forces:

$$F_{r1} = \frac{V}{\sqrt{gy}} \tag{2-5}$$

A hydraulic jump will occur if the downstream subcritical flow depth (y_3) satisfies Equation (2-4) (Forster & Skrinde, 1950). Therein lies the problem if a hydraulic jump is required at a certain location, such as a stilling basin, but cannot occur as one of the sequent depths is not satisfied at the desired location. An abrupt step is therefore introduced to influence the downstream flow depth and cause a hydraulic jump. The step introduces an upstream-directed force, which reduces the downstream momentum required for a jump to occur, as per Equation (2-1). Therefore, a similar analysis to the above regarding the simple hydraulic jump is used when an abrupt step is considered.

Forster and Skrinde (1950) took a similar approach to this in their analysis. They knew that through Equation (2-4), the sequent depth of the jump would be reliant on the Froude number. They then considered the new design aspects required when introducing an abrupt step, such as the step height (h) and the distance from the toe of the jump to the step (X) (Fig. 2-1). However, in their experiments they kept X constant and large enough to ensure a complete jump before the step (Forster & Skrinde, 1950). With this limitation, the general approach to determining a relationship that could be used in design was created. Other researchers including Hager and Sinniger (1985) and Hager and Bretz (1986) followed a similar relationship formulation, but altered features regarding the momentum function and pressure distribution.

Fig. 2-1 shows the general arrangement of the hydraulic jump when it is controlled by an abrupt step. Forster and Skrinde (1950) postulated that when using a step to control a hydraulic jump, the general form of the relationship should be:

$$\frac{h}{y_1} = f\left(Fr_1, \frac{y_3}{y_1}\right) \tag{2-6}$$

Due to the importance of the step in the flow, the researchers took the control section as between just before the step (section 2) and after the step (section 3) (Fig. 2-1). They then assumed hydrostatic pressure distribution at the abrupt step and calculated the force on the step as:

$$F = \frac{1}{2}\gamma h(2y_2 - h) \tag{2-7}$$

They then applied the momentum function equation (Equation (2-1)) together with Equation (2-7). However, due to the complexity of the flow depth at position 2 in front of the step, Forster and Skrinde (1950) used continuity with position 1 and eliminated y_2, V_2, and V_3. That produced:

$$\left(\frac{y_3}{y_1}\right)^2 = 1 + 2Fr_1^2\left(1 - \frac{1}{y_3/y_1}\right) + \frac{h}{y_1}\left(\frac{h}{y_1} - \sqrt{1 + 8Fr_1^2} + 1\right) \tag{2-8}$$

Equation (2-8) provides the relationship for the basic design parameters needed to ensure a stable hydraulic jump in a stilling basin, according to Forster and Skrinde (1950). The exact location of the jump relative to the step is unknown. However, the assumption that there was hydrostatic pressure distribution and uniform velocity distribution just before the step implies that the hydraulic jump is far enough upstream so that it is completed before the step. This is referred to as a type A hydraulic jump (Hager & Bretz, 1986). In Forster and Skrinde's (1950) experiments, the jump was set to a distance X away from the step by the ratio $5 = X/(h + y_3)$ for numerous step heights (h) to allow for a stable jump. The results compared well with Equation (2-8), but the X-value relationship could not be confidently used to predict the actual X value if used outside of their experiments. The researchers stated that if the ratio of $X/(h + y_3)$ was larger, then the experimental results would have been more accurate when comparing results from Equation (2-8) (Forster & Skrinde, 1950). Again this was due to the relationship formulation, and the assumptions that velocity distribution was uniform and that pressure was hydrostatic at the step.

Following on from Forster and Skrinde (1950), Hager and Sinniger (1985) revisited earlier work done on abrupt steps to force a hydraulic jump. Einwachter (1930) (as presented in Hager and Sinniger (1985)), unlike Forster and Skrinde (1950), did not use the flow depth at the step (y_2) in the formulation of a relationship. Instead, it was assumed that the flow depth at the step (y_2) minus the step height (h) was equal to the flow depth downstream (y_3) i.e. $y_2 - h \cong y_3$ (Fig. 2-1). Momentum was applied through the free body between sections 1 and 3.

Einwachter (1930) (as presented in Hager and Sinniger (1985)) also assumed hydrostatic pressure and uniform velocity distributions through the step and the following relationship was produced:

$$\frac{q^2}{gy_1} + \frac{y_1^2}{2} = \frac{q^2}{gy_3} + \frac{y_3^2}{2} + h\left(y_3 + \frac{h}{2}\right) \tag{2-9}$$

However, Hager and Sinniger (1985) did not agree that the pressure and velocity distributions were hydrostatic and uniform, respectively. They hypothesised that the pressure distribution would not be hydrostatic in front of the step and that y_2 is greater than y_3. That resulted in a pressure distribution greater than hydrostatic. Hager and Sinniger (1985) then stated that this pressure at the front of the step would likely depend on y_2, Fr_1, and the step geometry, but did not elaborate. The researchers then assumed that the pressure distribution was uniform (Fig. 2-5). With that new pressure distribution assumption, Hager and Sinniger (1985) adapted Equation (2-9) to:

$$\frac{q^2}{gy_1} + \frac{y_1^2}{2} = \frac{q^2}{gy_3} + \frac{y_3^2}{2} + h(y_3 + h) \tag{2-10}$$

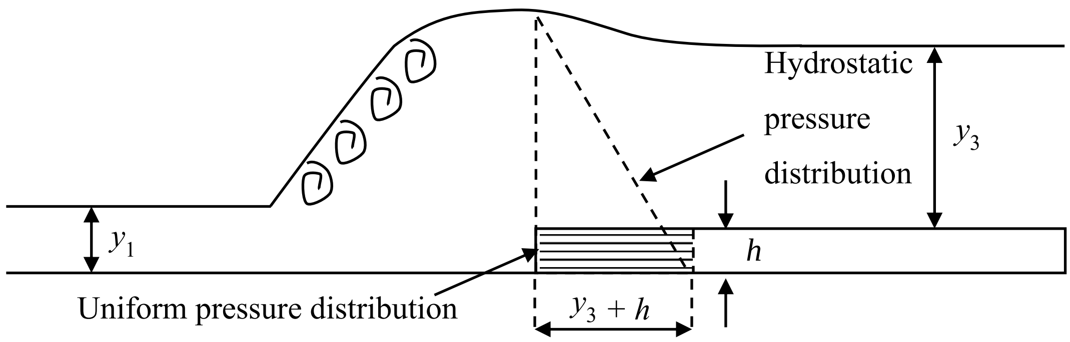

Figure 2-5- Pressure distributions on an abrupt step

The use of uniform pressure distribution by Hager and Sinniger (1985) was not justified, except for the fact that the pressure must be greater than hydrostatic pressure. Hager and Sinniger (1985) then used the experimental results from Forster and Skrinde's (1950) study and commented that Equation (2-9) agreed "fairly well" with the experiments. However in Forster and Skrinde's (1950) experiments, the toe of the jump was set far enough upstream to allow completion of the jump before the step. Consequently, this would imply that the pressure distribution in front of the step would tend toward hydrostatic.

A further study by Hager and Bretz (1986) provides greater clarity and distinction between Equations (2-9) and (2-10). The researchers first provided a subjective distinction between the different types of jumps that could occur through an abrupt step. An A-jump was described as a jump that is entirely located upstream of the step (Hager & Bretz, 1986) i.e. entirely in the stilling basin, or the length of the hydraulic jumps roller (L_r) ends at the step (Fig. 2-6). L_r or roller length of a jump, as defined by Hager and Bretz (1986) is the distance between the jump toe and the largest extent of the separation zone. The other jump type of interest is the B-jump, which is defined as having the jump's roller located partly upstream and downstream of the step (Hager & Bretz, 1986) (Fig.2-7).

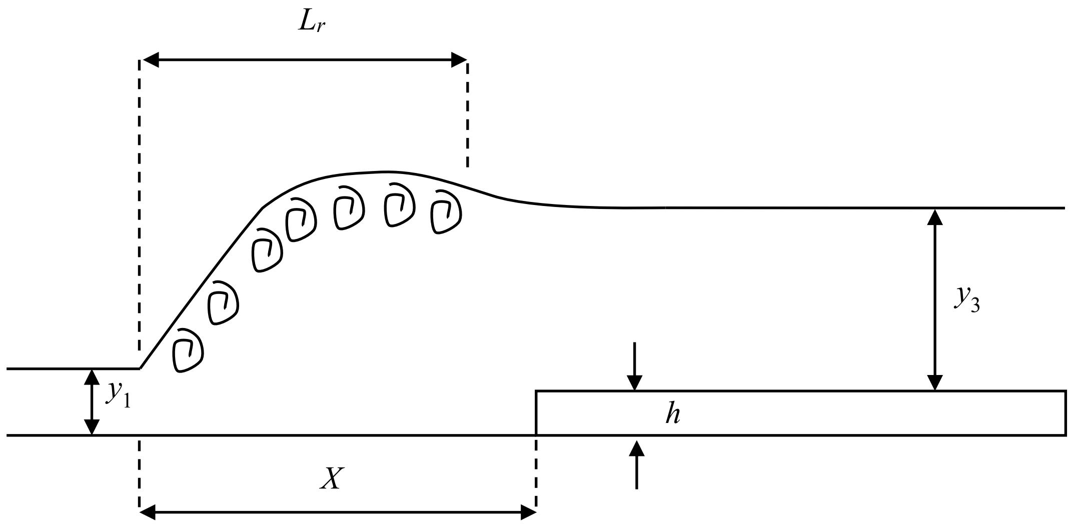

Figure 2-6- Type A hydraulic jump induced by a step

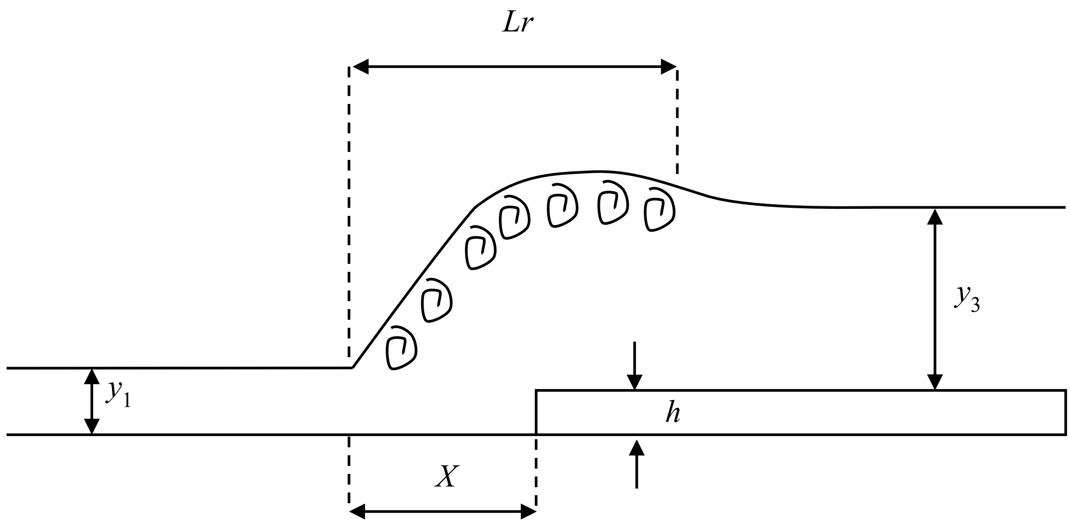

Figure 2-7- Type B hydraulic jump induced by a step

The researchers then assigned Equations (2-9) and (2-10) to the two hydraulic jump types. Equation (2-9) was assigned to A-jumps, while equation (2-10) was assigned to B-jumps. The logic behind assigning Equation (2-9) to A-jumps was sound as the researchers stated that A-jumps are characterised by nearly hydrostatic pressure and uniform velocity distributions at the step, which correlates with the jump being completely formed before the step. However, the researchers assumed that Equation

(2-10) corresponded to B-jumps and therefore also assumed that B-jumps had uniform pressure distribution at the step. This judgment was unfounded as no logical reasoning was given, besides the opinion that because the jump is closer to the step, the pressure distribution is not hydrostatic.

The main issues the three formulations (Equations (2-8), (2-9), and (2-10)) face are regarding the velocity and pressure distributions. Both these issues are debated comprehensively by other researchers in discussions to both Forster and Skrinde's (1950) and Hager and Sinniger's (1985) work.

Depending on the position of the hydraulic jump's toe in relation to the step, the uniformity of the flow at the step would decrease as the toe approaches the step (Forster & Skrinde, 1950). However, in the above relationships by Forster and Skrinde (1950), Hager and Sinniger (1985) and Hager and Bretz (1986), the sections considered when applying momentum through the step are sections 1 and 3 in the final equations. These sections are far enough upstream and downstream of the step that uniform velocity distribution is permissible (Forster & Skrinde, 1950). Therefore, momentum correction coefficients at sections 1 and 3 are not required.

The nonuniformity in the velocity distribution and pressure distribution at the step (section 2) is an issue. In Equations (2-8), (2-9), and (2-10) there is a term accounting for the force on the step relating to the flow conditions at the step (section 2). In Forster and Skrinde's (1950) equation development, the flow conditions at section 2 were eliminated through continuity. However, nonuniformity at the step (section 2) should be accounted for in the relationship (Forster & Skrinde, 1950). The effect of this nonuniformity also means that hydrostatic pressure does not occur at the step (Laushey, 1950). It was then proposed by Laushey (1950) that a dynamic component be added to Equation (2-8). This dynamic component would consider the drag on the step and the approach velocity (Laushey, 1950).

Considering these two aspects involved (a momentum correction and a dynamic component), a new relationship by Laushey (1950) was compared to Forster and Skrinde's (1950) experimental results. The results were more closely aligned with the experimental results, but the relationship still overestimated predicted results. Therefore, the improved results would not be justified as the process of obtaining the required additional terms would only produce minor improvements.

Similar attempts to improve Equation (2-9) by Hager and Sinniger (1985) were made by Fiuzat (1986), and Karki and Mishra (1986). Fiuzat (1986) considered that a stagnation point occurred at the bottom of the step and adjusted the force component in Equation (2-9) accordingly. Karki and Mishra (1986) did not agree with the use of uniform pressure distribution by Hager and Sinniger (1985) and proposed that an average flow depth be used between the flow depth at the step (y_2) and the flow depth downstream, with the step height ($y_3 + h$) in the calculation of the force on the step. This has practical limitations, especially for jumps close to the step (B-jumps), as y_2 is difficult to measure due to the turbulent flow at the step. Only slight improvements were made but, again, the new adjustments only made minor differences that still overestimated against the experimental results.

Interestingly, the position of the hydraulic jump's toe with respect to the step was only analysed qualitatively in the above research. Hager and Bretz (1986) differentiate between A- and B-jumps and assign equations to those jumps respectively. However, greater significance should be placed on the exact location of the jump as the velocity and pressure distributions are affected by the position of the jump relative to the step, influencing the important design parameters.

2.2.2. Position of the hydraulic jump

Depending on the type of design needed when utilising an abrupt step, an A-jump or B-jump is chosen. An A-jump requires a longer stilling basin while a B-jump is more compact in front of the step and requires a shorter basin. However, the B-jump roller will extend past the step downstream and will require a longer section of erosion protection after the step (Hager & Bretz, 1986).

Using the length of the roller of the hydraulic jump (L_r), Hager and Bretz (1986) produced two relationships that predicted the lengths of the two different jumps types. For A-jumps:

$$L_r \cong 4.75(y_3 + h) \tag{2-11}$$

and for B-jumps:

$$L_r \cong 4.25(y_3 + h) \tag{2-12}$$

In Hager and Bretz's (1986) study, the roller for B-jumps extended $L_r/2$ upstream and $L_r/2$ downstream of the step. Equations (2-11) and (2-12) were approximate and the researchers mentioned that no definitive trend was perceptible when determining these equations (Hager & Bretz, 1986).

Hager and Sinniger (1985) also provided an approximation for the length of a roller when using an abrupt step. However, their relationship (with reliance on data from Einwachter (1930), Safranez (1929), Schröder (1957), Peterka (1983), Rajaratnam (1965) and Woycicki (1931)) was developed using jump lengths in horizontal, prismatic rectangular channels and adapted by accounting for the step (Hager & Sinniger, 1985). The relationship produced also utilised the downstream depth (y_3) and the step height (h) and was presented as:

$$L_r \cong 4.5\left(y_3 + \frac{6h}{5}\right) \tag{2-13}$$

The hydraulic jump roller length produced by Equation (2-13) can be used as the limit for B-jumps in a basin. If the distance from the toe of the jump to the step (X) is less than L_r, then the jump is classified as a B-jump and if X is larger than L_r, then it is an A-jump.

Although the length of the roller of the hydraulic jump has been defined, the actual distance from the toe of the jump to the step (X) has not. Considering the importance of the location of the jump, the distance should be a vital design factor.

Hager and Li (1992) developed a relationship that incorporated the distance between the toe of a hydraulic jump and a vertical sill. A vertical sill is a nonaerated weir with a sharp crest (Forster & Skrinde, 1950). The empirical relationship adjusted the sequent depth ratio of a simple hydraulic jump in a horizontal, prismatic rectangular channel (Equation (2-4). The adjustments accounted for the effect of wall friction and the effect of the sill. The adjustment, due to the effect of the sill (ΔY_s), is of interest as it was established that it was a function of the ratio of sill height (h_s) to incoming flow depth (y_1). The ratio of the distance between the toe of the jump and sill (X_s), and the roller length of a simple hydraulic jump (L_r^*) also affects ΔY_s. The basic function form being:

$$\Delta Y_s = f\left(\frac{h_s}{y_1}, \frac{X_s}{L_r{}^*}\right) \tag{2-14}$$

The final equation developed to determine the new sequent depth ratio was:

$$Y = Y^* - \Delta Y_s - \Delta Y_f \tag{2-15}$$

where

Y = Sequent depth ratio due to the sill

Y^* = Sequent depth ratio of a simple hydraulic jump (Equation (2-4))

ΔY_s = Adjustment due to the sill

ΔY_f = Adjustment due to friction

Although this method was developed using a vertical sill, the same logic could be applied to abrupt steps.

2.3. Hysteresis

In open channel flow, when supercritical flow approaches an obstacle, a phenomenon called hydraulic hysteresis can occur (Viero & Defina, 2017). For particular incoming flow characteristics that occur on an obstacle, multiple stable flow states can occur depending on the history of the flow (Viero & Defina, 2017). Hysteresis has been widely investigated with several obstacles such as sluice gates, steps, and channel constrictions.

As the design of steps in stilling basins is of interest, this review investigates hysteresis regarding both abrupt and sloping steps. The occurrence of hysteretic flow through a step could have significant design implications as the two stable states are when the hydraulic jump occurs downstream of the step or when it occurs upstream of the step. When it occurs downstream of the step it is called sweep-out, which is undesirable due to its erosive effect on the channel bed. When the jump occurs upstream of the step, it may occur at a distance that is greater than the length of the stilling basin, which is also undesirable.

Early research on hysteretic flow behaviour through steps was conducted by Muskatirovic and Batinic (1977) and Defina and Susin (2006). However, these studies only placed emphasis on the incoming supercritical flow. A later study by Viero and Defina (2017) considered hysteresis on a step in terms of the incoming supercritical flow, as well as the subcritical flow that was controlled further downstream. Viero and Defina (2017) produced two theoretical approaches for determining the hysteretic limits. The first method uses specific energy conservation through a step and the second approach uses momentum conservation through the step.

The first method, although referred to as the specific energy approach, also uses momentum conservation, however the momentum conservation does not occur through the step. Specific energy is defined as the total energy of the flow relative to the bed (Chadwick, et al., 2013). Therefore, it can be defined as the sum of the velocity head and the flow depth:

$$E = y + \frac{V^2}{2g} \tag{2-16}$$

where

E = Specific energy (m)

y = Flow depth (m)

V = Velocity (m/s)

g = Gravitational acceleration (9.81 m/s^2)

Momentum conservation uses the momentum function, which for rectangular channels can be expressed per unit width as Equation (2-2)

As mentioned, there are two stable states that can occur for the same flow configuration. The first stable state occurs when the incoming supercritical flow passes over the step and the hydraulic jump occurs downstream (Fig. 2-8).

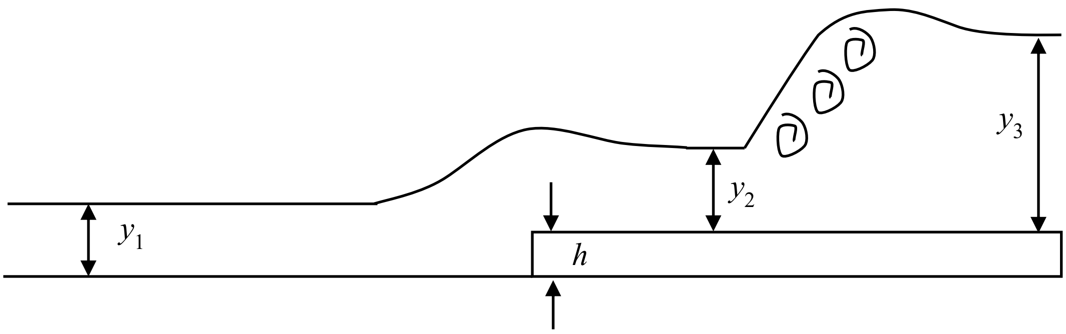

Figure 2-8- Hydraulic jump downstream with supercritical flow over the step

In order for Fig. 2-8 to occur, Viero & Defina (2017) proposed that the incoming supercritical flow (y_1) must first have enough energy to be able to pass over the step:

$$E_1 - (E_{loss} + h) \geq E_c \tag{2-17}$$

where

E_1 = Specific energy at section 1 (m)

E_{loss} = Energy loss over the step due to the step (m)

E_c = Specific energy for critical flow, the minimum required to pass over the step (m)

Just after it has passed over the step, the supercritical flow after the step (y_2) must have equal to or greater momentum than the sequent flow depth of the downstream subcritical flow (y_3):

$$M_2 \geq M_3^* \quad (2\text{-}18)$$

where

M_2 = Momentum at section 2 (m^2/m)

M_3^* = Momentum of the sequent depth of the downstream flow y_3 (m^2/m)

If y_2 has greater or equal momentum than the sequent depth of the y_3, then sweep-out will occur as the only stable state. If M_2 is greater than or equal to M_3^*, this implies that y_2 is less than or equal to y_3^*, which means E_2 must be greater than or equal to E_3^*:

$$y_2 \leq y_3^* \quad (2\text{-}19)$$

which also means:

$$E_2 \geq E_3^* \quad (2\text{-}20)$$

However, E_2 and the energy losses due to the step and energy dissipation (E_{loss} and h) are equal to E_1. Therefore:

$$E_1 \geq E_3^* + (E_{loss} + h) \quad (2\text{-}21)$$

This is referred to as the lower boundary condition by (Viero & Defina, 2017).

The next stable state that can occur is when subcritical flow happens upstream of the step (Fig. 2-9).

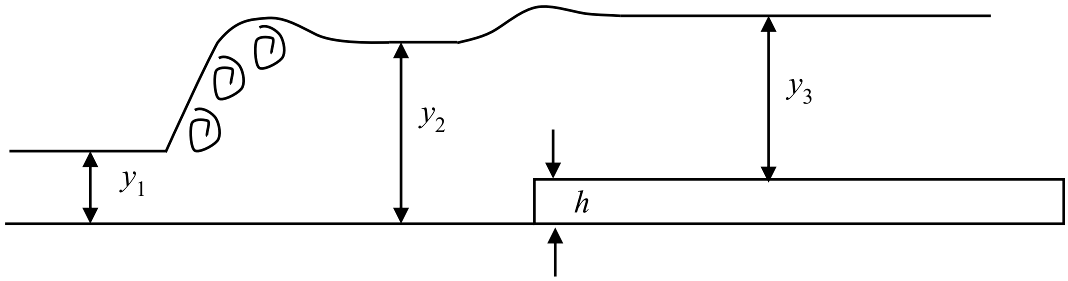

Figure 2-9- Hydraulic jump upstream with subcritical flow over the step

For Fig. 2-9 to occur, the following must be satisfied. Just as the hydraulic jump enters the basin and occurs just before the step, then the supercritical sequent depth (y_2^*) must have equal or greater momentum than the upstream supercritical (y_1):

$$M_1 \leq M_2^* \tag{2-22}$$

This again implies that y_2^* is less than y_1, which means E_2^* is greater or equal to E_1:

$$E_1 \leq E_2^* \tag{2-23}$$

Viero & Defina (2017) refer to the inequality in Equation (2-23) as the upper limit. For this to be related to the downstream subcritical flow (y_3), the subcritical flow in front of the step (y_2), which is related to y_2^* through momentum, must have the same specific energy as E_3 and the energy losses due to the step and energy dissipation (ΔE). Therefore:

$$M_2 = M_2^* \tag{2-24}$$

From which, y_2 is known and therefore E_2. Then:

$$E_2 = E_3 + (E_{loss} + h) \tag{2-25}$$

Finally, putting both limits from Equations (2-21) and (2-23) together,

$$E_3^* + (E_{loss} + h) \leq E_1 \leq E_2^* \tag{2-26}$$

In-between these two limits the theoretical hysteresis zone exists. Two stable states can occur, however the one that forms depends on the history of the flow.

Viero and Defina (2017) then define the second approach using momentum conservation over the step. However, the researchers do not advocate the approach as the curvature of the streamlines across the step are severe and the pressure is not hydrostatic (Viero & Defina, 2017). Therefore, the forces on the step cannot be accurately determined.

Firstly, when supercritical flow occurs over the step, the momentum at section 2 is equal to the momentum at section 1 upstream less the resistive force imposed by the step ($P_{supercritical}$):

$$M_2 = M_1 - P_{supercritical} \tag{2-27}$$

Conversely, when subcritical flow occurs over the step, the momentum at section 3 is equal to the momentum at section 2 less the resistive force imposed by the step ($P_{subcritical}$):

$$M_3 = M_2 - P_{subcritical} \tag{2-28}$$

For there to be supercritical to flow over the step, M_2 must be equal to or greater than M_3:

$$M_2 \geq M_3 \tag{2-29}$$

Substituting Equations (2-27) and (2-28) into (2-29) then yields:

$$M_1 \geq M_2 - P_{subcritical} + P_{supercritical} \tag{2-30}$$

For there to be subcritical flow over the step, M_2 must be equal to or greater than M_1:

$$M_1 \leq M_2 \tag{2-31}$$

Finally, according to Viero and Defina (2017), the dual solution limits are:

$$M_2 - P_{subcritical} + P_{supercritical} \leq M_1 \leq M_2 \tag{2-32}$$

Due to the difficulty in determining the resistance caused by the step ($P_{subcritical}$ and $P_{supercritical}$), the energy approach is preferred by Viero and Defina (2017). However, in the energy approach, the energy losses due to the step and energy dissipation (E_{loss} + h) are very important. If the energy losses due to energy dissipation are neglected, an obvious hysteresis region exists. But if the losses due to energy dissipation through the step are included, the hysteresis region shrinks. For abrupt steps, if energy losses are included, Viero and Defina (2017) state that the region shrinks to one limit and no dual stable state exists.

Viero and Defina (2017) carried out some arithmetic manipulation on the energy approach's hysteresis limits in Equation (2-26) to express the limits in terms of h/y_1. Fig. 2-10 shows an example used by Viero and Defina (2017) depicting the hysteresis region in terms of h/y_1 and F_{r3} for a constant F_{r1} (where F_{r1} was equal to 4).

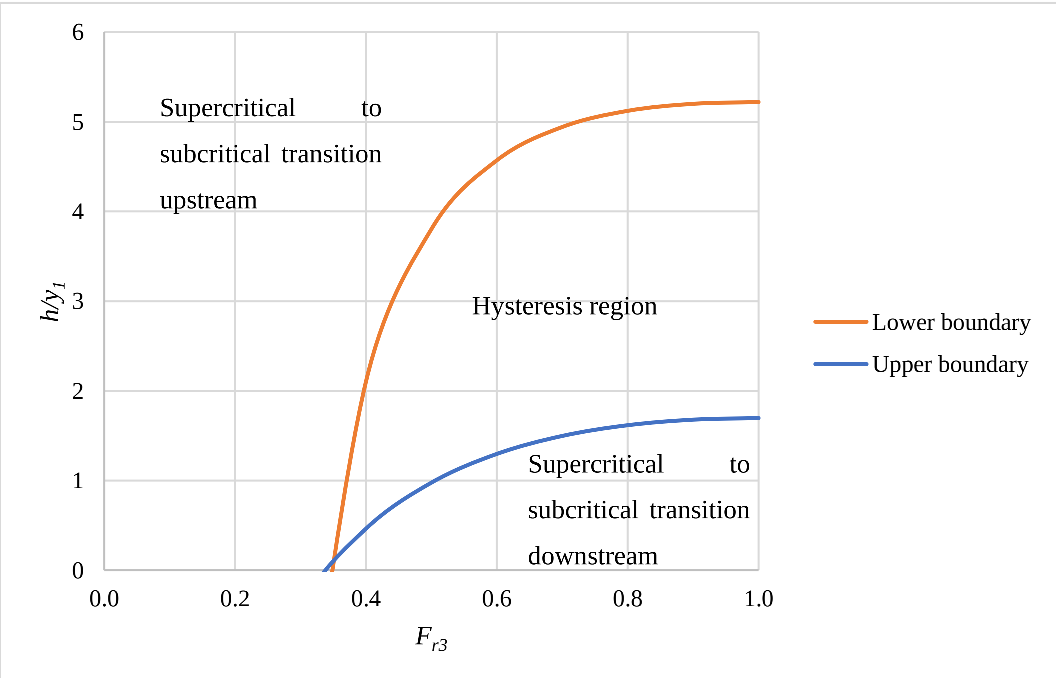

Figure 2-10- An example by Viero and Defina (2017) showing the lower and upper limits of the hysteresis region when F_{r1} is 4 for h/y_1 and F_{r3}

From Fig 2-10, there are three distinct regions: supercritical to subcritical transition upstream (hydraulic jump in front of the step), hysteresis region, and supercritical to subcritical transition downstream (sweep-out). At h/y_1 equal to 1, if F_{r3} started in-between 0 and 0.35, the hydraulic jump would be situated upstream. If F_{r3} were to increase above 0.35, the jump would now be in the hysteresis zone. However, because the state of the flow started with the jump in the upstream position, it would stay in that state. If F_{r3} were increased above 0.50, the hydraulic jump would sweep-out and the jump would be downstream of the step. Now, if F_{r3} were to decrease below 0.5, the jump would stay in the sweep-out position as this was the previous state of the flow before it entered the hysteresis zone. Therefore, there are values of F_{r3} that would have experienced both states, but their governing state depends on the history of the flow.

An interesting observation was made by Viero and Defina (2017) where for a given F_{r1}, and when h/y_1 is sufficiently large, a hydraulic jump downstream would be able to move upstream of the step if y_3 is increased, thus reducing F_{r3}. But the jump cannot move back downstream if y_3 is decreased, hence increasing F_{r3}. This could have important design implications. This is shown in Fig. 2-10 if h/y_1 is greater than approximately 1.80. However, as the hysteresis region shrinks to one line for abrupt steps (Viero & Defina, 2017), this finding does not apply.

In Viero and Defina’s (2017) study, the effect of the position of the jump was not investigated, nor the effect of the sequent depth ratio. Both these characteristics could have important design implications when designing for a step height in a stilling basin.

2.4. Objectives

In the review of the literature regarding abrupt step design, it is shown that the established design elements are the step height (h) and the flow depths of the hydraulic jump upstream and downstream of the step. When determining these design elements, knowing the force on the step is essential. The uncertainty in determining this force is clear and has been greatly discussed in the literature. The location of the hydraulic jump influences this force, but is not accounted for in the design relationships by Forster and Skrinde (1950), Hager and Sinniger (1985), and Hager and Bretz (1986). An empirical method by Hager and Li (1992), using a different energy dissipating structure (a sill), utilised the position of the hydraulic jump in the design relationship.

The current study examines the importance of the distance from the toe of the hydraulic jump to the abrupt step (X) in the design of an abrupt step stilling basin. X is important as it defines the basin length to be designed. This study will focus on B jumps, due to the complexities in the pressure and velocity distributions. It will also examine the importance of the sweep-out condition and provide a limitation when designing a step.

Following the research done by Viero and Defina (2017), this study also examines the effect of hysteresis in the design of a stilling basin utilising a step. Although sloping steps would not be used in real-world applications due to the decrease in the energy dissipation caused by the slope and therefore the tendency to sweep-out, both sloping and abrupt steps are investigated to conduct a holistic study.

3. Experimental methodology

3.1. Introduction

The experimental investigation was conducted in the hydraulics laboratory in the School of Civil and Environmental Engineering at the University of the Witwatersrand. All the experiments took place in a single 3.0 m long, 0.10 m wide flume (Fig. 3-1) within the laboratory. The flume used a fixed volume of water stored in a tank. The water was continually recycled through the system by a Whisperflo 150 pump (Fig. 3-2). The pump had a single power output that remained constant. A standard adjustable valve was used to control the volume of water through the system (Fig. 3-3). The discharge could then be measured and read off an electronic gauge (Fig. 3-4). Affixed to the end of the flume was an adjustable end weir (Fig. 3-5). The flume's slope could be adjusted but for the experimental work carried out, the slope was kept at zero. The flume has a linear length scale to allow the accurate placing of equipment and objects. A detailed schematic of the laboratory flume is shown in Fig. 3-6. Additional equipment was used during testing and is described in the following section.

Figure 3-1- Photograph of entire laboratory set up

Figure 3-2- Whisperflo 150 pump

Figure 3-3- Discharge control valve

Figure 3-4- Electronic discharge gauge

Figure 3-5- Adjustable tail weir

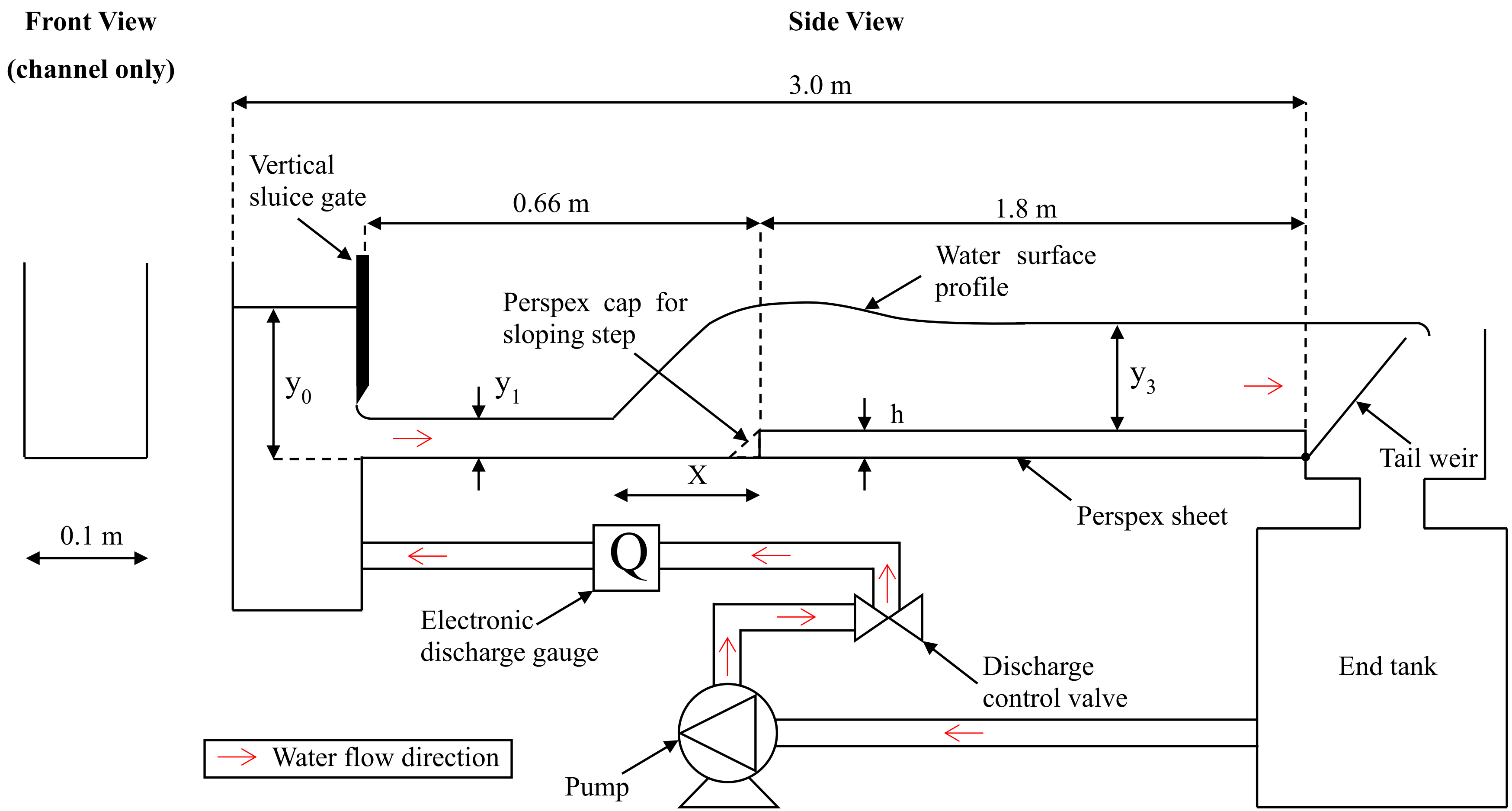

Figure 3-6- Schematic of the flume used in the experiments (not to scale)

3.2. Equipment

The following equipment was made available by the laboratory and used in the experimental investigation:

- Vertical sluice gate, with adjustable height and position along the flume (Fig. 3-7)
- Digital pointer gauge to measure vertical flow depth along the length of the flume (Fig. 3-8)

Figure 3-7- Vertical sluice gate

Figure 3-8- Digital pointer gauge

3.3. Materials

Two experimental set-up types were needed for the investigations of the abrupt step and hysteresis testing, which included abrupt and sloping steps. For both set-ups, a false bottom was created to simulate a positive step. Fig 3-9 shows a general schematic of the sheets of Perspex used to create the steps.

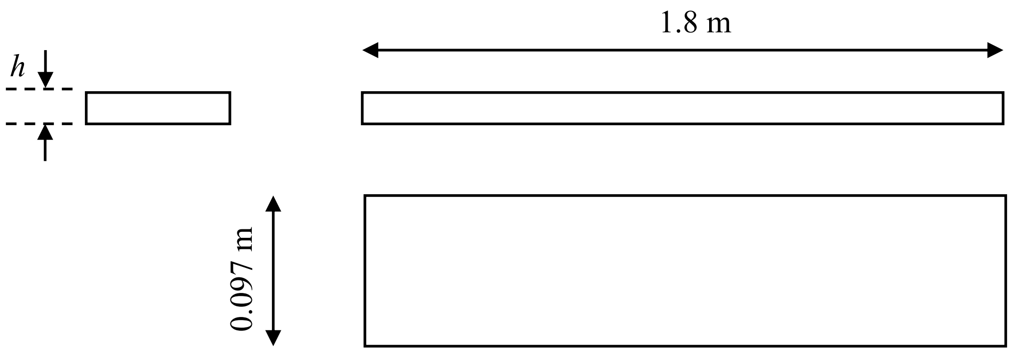

Figure 3-9- General schematic of Perspex sheeting used in the experiments (not to scale)

For the abrupt step experiments, five different step heights (*h* in Fig. 3-2) were tested: 5 mm, 10 mm, 15 mm, 20 mm, and 25 mm. To configure the different abrupt step set-ups, three sheets of Perspex were required. The three sheets all had the same length and width dimensions of 1.8 m and 0.097 m but different thicknesses with dimensions of 5 mm, 10 mm, and 15 mm. The 20 mm and 25 mm steps were assembled by superimposing the 5 mm sheet on the 15 mm sheet and the 10 mm sheet on the 15 mm sheet, respectively. 5 mm thin pieces of Perspex were used to cap the double sheet steps and create a uniform step.

The sloping step experiments were carried out using only the 10 mm Perspex step height. Four slopes were tested: 1-in-1, 1-in-2, 1-in-3, and 1-in-4. The slopes were created as attachments to the 10 mm abrupt step height. They were made by filing down thin sheets of Perspex to the angle of the required slope.

Finally, to place the sheets of Perspex securely and seamlessly into the flumes, Bostik clear silicone sealant was used. The silicone was also used to attach the thin capping Perspex pieces for the double sheet steps and attach the sloping steps to the 10 mm step height sheet.

3.4. Preliminary checks

Two preliminary checks were conducted in the flume before testing was carried out. The first inspected the accuracy of the electronic discharge gauge and the second inspected the range of the incoming Froude number available during testing.

The electronic discharge was checked using the vertical sluice gate in the flume with no other objects placed in the flume. With the flume operating, a constant discharge was set on the electronic gauge and the water level behind the sluice gate and the flow depth just in front of the gate were measured. The specific energy principle was applied across the gate to determine the discharge. Fig. 3-3 below compares the electronic gauge discharge with the specific energy discharge. The absolute relative percentage error was 2.83%, which is satisfactory.

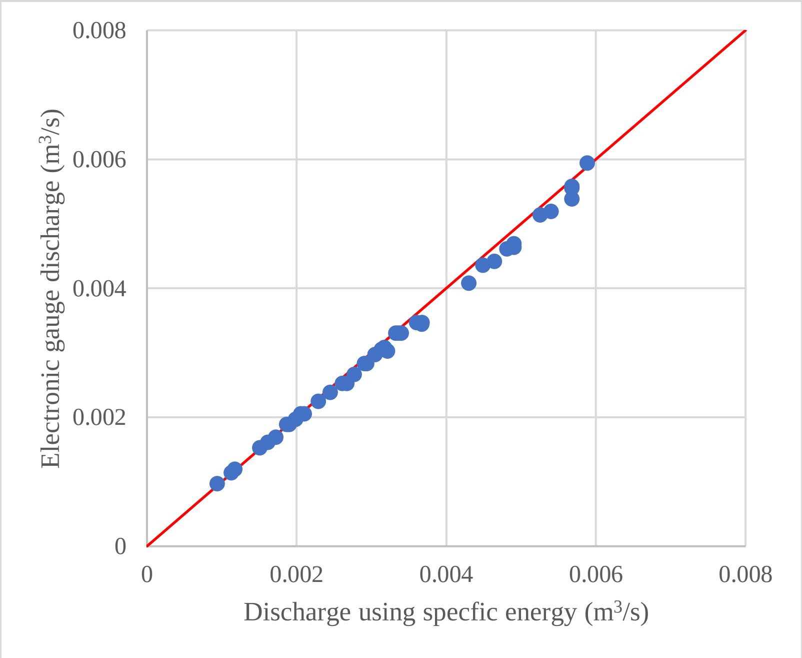

Figure 3-10- Comparison between the electronic discharge and the specific energy discharge

The second check involved establishing the Froude number range for supercritical flow being released from the vertical sluice in the flume. The vertical sluice gate only allowed certain maximum water levels behind the gate due to its height. There was a minimum gate height available for different discharges, therefore there was a resulting maximum Froude number. Fig. 3-4 was created and shows the range of incoming Froude numbers to be between 3 and 11 for the discharges available.

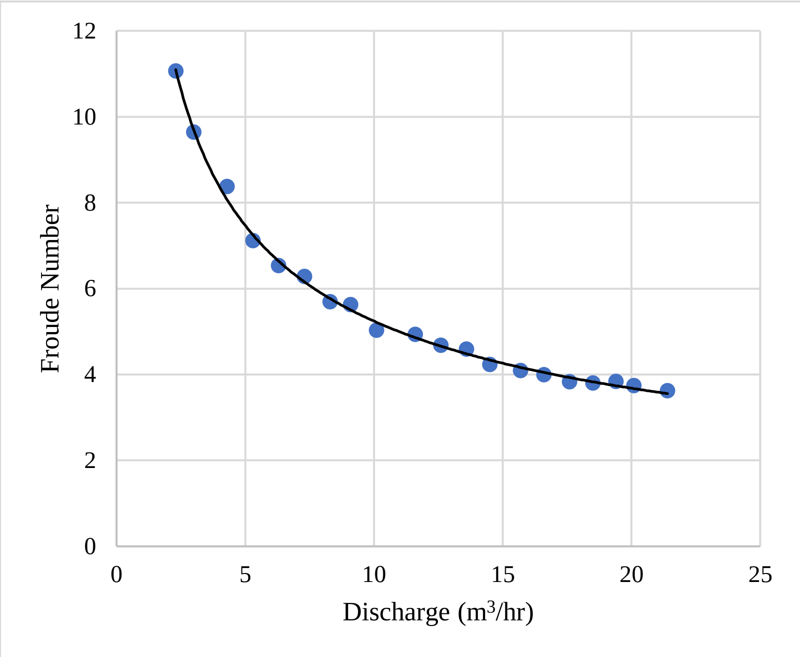

Figure 3-11- Maximum available Froude number for a given discharge

3.5. Experimental procedure

There were two main sets of experiments: abrupt step experiments and hysteresis experiments. The procedures for both sets were as follows:

3.5.1. Abrupt step

Depending on the step height, the Froude number (F_{r1}) was varied between 3 and the maximum allowed for the set-up.

Each run was differentiated by Froude number, with multiple measurements made depending on the hydraulic jump location. The procedure for each run was as follows:

1) A run started with a hydraulic jump downstream of the step and the downstream flow depth at its lowest. A Froude number was selected within the desired range.
2) The flow depth upstream of the vertical sluice gate (y_0), flow depth just after the vertical sluice gate (y_1) and the flow depth just after the step (y_3) were recorded.
3) The tail weir was adjusted to increase the downstream flow depth therefore the hydraulic jump moved upstream toward the step.
4) Just before the jump moved upstream of the step, the flow depth, y_3, was recorded again.
5) The y_3 was increased further to allow the toe of the jump to move in front of the step.
6) The flow depth after the step (y_3) and the distance of the hydraulic jump toe from the step were measured (X).
7) The flow depth (y_3) was incrementally increased with the jump's toe position increasing simultaneously. With each increment, y_3 and X were measured until the jump's toe submerged the sluice gate.
8) The y_3 flow depth at submergence was recorded and the test run ended.

Once all the available Froude numbers for the current step height were tested, the next step height was placed in the flume.

3.5.2. Hysteresis

As mentioned, only the 10 mm step height was investigated in the hysteresis testing. Five set-ups were examined, including four sloping steps (1-in-1, 1-in-2, 1-in-3, and 1-in-4) and a 10 mm abrupt step. The incoming Froude number was varied between 4 and 10.

Each run for each set-up was differentiated by the incoming Froude number (F_{r1}), with multiple measurements made depending on the starting condition and hydraulic jump location. The first half of each test run was the same as for the abrupt step testing, however the tailwater was lowered after the jump submerged the vertical sluice gate and measurements were taken until the jump swept-out. The full procedure for each run was as follows:

1) Each run started with the hydraulic jump downstream of the step and the tail weir at its lowest position. A Froude number was selected within the allowable range.
2) The flow depth upstream of the vertical sluice gate (y_0), flow depth just after the vertical sluice gate (y_1), and flow depth just after the step (y_3) were recorded.
3) The tail weir was adjusted to increase the downstream flow depth (y_3). Therefore, the hydraulic jump moved upstream toward the step.
4) Just before the jump moved upstream of the step, the flow depth, $y_{3,}$ was recorded again.
5) y_3 was increased further to allow the toe of the jump to move in front of the step.
6) The flow depth after the step (y_3) and the distance of the hydraulic jump toe from the step was measured (X).
7) The flow depth (y_3) was increased incrementally with the jump's toe position increasing simultaneously. With each increment, y_3 and X were measured until the jump's toe submerged the sluice gate.
8) Differing from the abrupt step testing, after the sluice gate was submerged, the tail weir and therefore downstream flow depth was lowered until the jump downstream from the gate became unsubmerged.
9) The flow depth (y_3) was decreased incrementally with the jump's toe position decreasing simultaneously. With each increment, y_3 and X were measured until the hydraulic jump swept-out the basin.

Once all the available Froude numbers for the current set-up were tested, the next set-up was placed in the flume.

4. Abrupt step experiment analysis

The abrupt step results analysis is split into two parts: Location of the hydraulic jump, and Sweep-out limit. The analysis includes methodology, results, and discussion for both parts.

4.1. Location of the hydraulic jump

In previous studies, the location of the jump was only briefly explored. In this study, the effect of the distance between the hydraulic jump toe and the step was considered in the design of an abrupt step stilling basin.

4.1.1. Analysis methodology

From the five abrupt step heights tested, 248 data points were captured (Appendix A). The 5 mm height data were discarded as they conflicted with the data produced from the other four step heights. The conflict was attributed to the weak interaction between the step height and flow. The flow depth required for the 5 mm step needed to be shallow to allow adequate interaction, but the shallow flow resulted in a stronger surface bed friction influence.

Only data where the hydraulic jump's toe was in-between the vertical sluice gate and the step were considered. The data were then split by jump type, A-jump or B-jump. The jump types were classified by comparing the measured distance X to the roller length (L_r) given by Hager and Sinniger's (1985) roller length formula in Equation (4-1).

$$L_r \cong 4.5\left(y_3 + \frac{6h}{5}\right) \tag{4-1}$$

If the distance X was greater than the L_r from Equation (4-1), then it was classified as an A-jump and if it were smaller than L_r, then it was classified as a B-jump. The resulting B-jump data from the four remaining step heights were then randomly split in half. One half of the data was used for relationship development, while the other half was left as clean data for confirmation. Four relationships for predicting the distance of the jump toe from the step were developed from the same randomly selected 50% of the data. An additional relationship was developed only using 30% of the B-jump data. This selection was not random as the data was grouped according to the incoming Froude number (F_{r1}). This selection was used in the development of the 5th relationship.

For the development of relationships 1 to 4 below, multiple regression analyses where carried out using Microsoft Excel's Data Analysis tool. The Regression analysis tool performs linear regression analysis utilising the "least squares" method to fit a line through a set of observations (Microsoft, 2020). The least squares method determines the best approximating function when the error involved is the sum of the squares of the differences between the dependant values on the approximating function and the given dependant values (Burden & Faires, 2011). Microsoft Excel allows multiple independent variables to be analysed and determines how they affect a single dependant variable. In regression analysis, the coefficient of determination (R^2) is commonly used as a convenient indicator that shows how well the dependent and independent variables correlate. R^2 shows the adequacy of the regression model, where R^2 equal to 1 indicates a strong correlation and 0 indicates no correlation (Montgomery & Runger, 2011). As multiple independent variables are used in the regression of relationships 1 to 4, Microsoft Excel produced an adjusted coefficient of determination, which is used to describe the strength of the relationships. The same principle applies as above, adjusted R^2 equal to 1 indicates a strong correlation and 0 indicates no correlation.

4.1.2. Results

Five relationships were produced using the data selected for relationship development. The relationships are as follows:

4.1.2.1. Relationship 1 – sequent depth ratio and Froude number

The first relationship developed used the sequent depth ratio and the incoming Froude number as the independent terms. The subject of the relationship was the distance X from the toe of the jump to the step, normalised by the step height (h). The form of the relationship is:

$$\frac{X}{h} = f\left(\frac{y_3}{y_1};\ F_{r1}\right) \tag{4-2}$$

A multiple regression analysis was used to develop the relationship using Microsoft Excel's regression data analysis tool. The resulting relationship produced was

$$\frac{X}{h} = 19.3\left(\frac{y_3}{y_1}\right)^{5.19}(F_{r1})^{-4.88} \tag{4-3}$$

The adjusted coefficient of determination (R^2), accounting for both independent variables, was 0.805.

4.1.2.2. Relationship 2 – Sequent depth correction and Froude number

The second relationship developed used the sequent depth ratio correction and incoming Froude number as the independent terms. The sequent depth ratio correction was produced by calculating the sequent depth ratio of a simple hydraulic jump in a rectangular channel $\left(\frac{y_3{}^*}{y_1}\right)$ using Equation (2-4). The actual sequent depth produced when using a step from the experiments was then divided by $\frac{y_3{}^*}{y_1}$:

$$Y_{corr} = \frac{y_3}{y_1} \Big/ \frac{y_3{}^*}{y_1} \tag{4-4}$$

The form of the relationship was the same as relationship 1, however the sequent depth ratio was replaced with Y_{corr}:

$$\frac{X}{h} = f(Y_{corr};\ F_{r1}) \tag{4-5}$$

A multiple regression analysis was performed, resulting in the following relationship:

$$\frac{X}{h} = 47.3(Y_{corr})^{5.13}(F_{r1})^{0.623} \tag{4-6}$$

The adjusted coefficient of determination (R^2), accounting for both independent variables, was 0.801.

4.1.2.3. Relationship 3 – Force correction and Froude number

The third relationship developed used the correlation between the force on the step and the jump distance away from the step. As initially discussed by Forster and Skrinde (1950), and further by Hager and Bretz (1986), for an A-jump in a basin with a step, the velocity distribution and pressure distributions are assumed to be uniform and hydrostatic, respectively. These distributions are assumed to be different as the toe of the hydraulic jump approaches the step and the jump is classified as a B-jump. A force correction term was then created by comparing the idealised hydrostatic force on the step with actual force on the step. The actual force (P) on the step was calculated by the difference in momentum function between the upstream (y_1) and downstream (y_3) depths through the step, according to Equation (2-1). The actual force on the step (P):

$$\frac{P}{\gamma} = M_1 - M_3 \tag{4-7}$$

where

P = Force on the step per unit width (N/m)

γ = Unit weight of water (9810 kg m^{-2}s^{-2})

$M_{1,3}$ = Momentum (m^2/m)

The idealised hydrostatic force on the step:

$$\frac{F_{hydrostatic}}{\gamma} = h\left(y_3 + \frac{h}{2}\right) \tag{4-8}$$

Finally, the force correction (F_{corr}) was developed by dividing Equation (4-7) by Equation (4-8):

$$F_{corr} = \frac{P}{\gamma} \Big/ \frac{F_{hydrostatic}}{\gamma} = \left(\frac{q^2}{gy_1} + \frac{y_1^2}{2} - \frac{q^2}{gy_3} - \frac{y_3^2}{2}\right) \Big/ h\left(y_3 + \frac{h}{2}\right) \tag{4-9}$$

Similar to the previous relationships, the form of relationship 3 is:

$$\frac{X}{h} = f(F_{corr};\ F_{r1}) \tag{4-10}$$

A multiple regression analysis was performed, resulting in the following relationship:

$$\frac{X}{h} = 3.74(F_{corr})^{-1.56}(F_{r1})^{1.32} \tag{4-11}$$

The adjusted coefficient of determination (R^2), accounting for both independent variables, was 0.258.

4.1.2.4. Relationship 4 – Principles from Hager and Li (1992)

Hager and Li (1992) developed a method to determine the sequent depth ratio of a hydraulic jump through a vertical sill. The method used the sequent depth ratio of a simple hydraulic jump and adjusted it due to the sill and friction. The equation developed was:

$$Y = Y^{*} - \Delta Y_s - \Delta Y_f \tag{4-12}$$

where

Y = Sequent depth ratio due to the sill = $\frac{y_3}{y_1}$

Y^{*} = Sequent depth ratio of a simple hydraulic jump = $\frac{{y_3}^{*}}{y_1}$

ΔY_s = Adjustment due to the sill = $\mathrm{f}\left(\frac{\mathrm{h_s}}{\mathrm{y_1}}, \frac{\mathrm{X_s}}{\mathrm{L_r}^{*}}\right)$

ΔY_f = Adjustment due to friction

For the fourth relationship, Equation (4-12) was adjusted to allow the subject of the formula to be $\frac{X_s}{{L_r}^{*}}$, where X_s is X for an abrupt step. Y^{*} subtracted from Y is called the sequent ratio difference (Y_{diff}). The sill height (h_s) is the abrupt step height (h). Finally, adjustments due to friction were omitted as they are assumed negligible. Therefore, the functional form produced was:

$$\frac{X}{{L_r}^{*}} = f\left(Y_{diff}; \frac{h}{y_1}\right) \tag{4-13}$$

A multiple regression analysis was performed using these variables and the resulting relationship produced was:

$$\frac{X}{{L_r}^{*}} = -0.253 Y_{diff} + 0.440 \frac{h}{y_1} + 0.680 \tag{4-14}$$

The adjusted coefficient of determination (R^2), accounting for both independent variables, was 0.434.

In order to compare the results of all the relationships, the results from Equation (4-14) were converted to X/h. This requires determining the roller length (L_r^*) of the simple hydraulic jump and then dividing it by the step height (h). L_r^* was predicted using empirical relationships proposed by Hager et al. (1990). The roller length was found to be dependent on the Froude number of the incoming flow. If the Froude number was greater than 8, the roller length was found to depend on the Froude number and the ratio of the incoming flow depth (y_1) divided by the width of the channel (b).

For $2.5 < F_{r1} < 8.0$:

$$\frac{L_r^*}{y_1} = 8(F_{r1} - 1.5) \tag{4-15}$$

For $F_{r1} > 8.0$ and $y_1/b < 0.10$:

$$\frac{L_r^*}{y_1} = -12 + 160 tanh\left(\frac{F_{r1}}{20}\right) \tag{4-16}$$

For $F_{r1} > 8.0$ and $y_1/b > 0.10$:

$$\frac{L_r^*}{y_1} = -12 + 100 tanh\left(\frac{F_{r1}}{12}\right) \tag{4-17}$$

Equations (4-15) to (4-17) are presented in Fig. 4-1

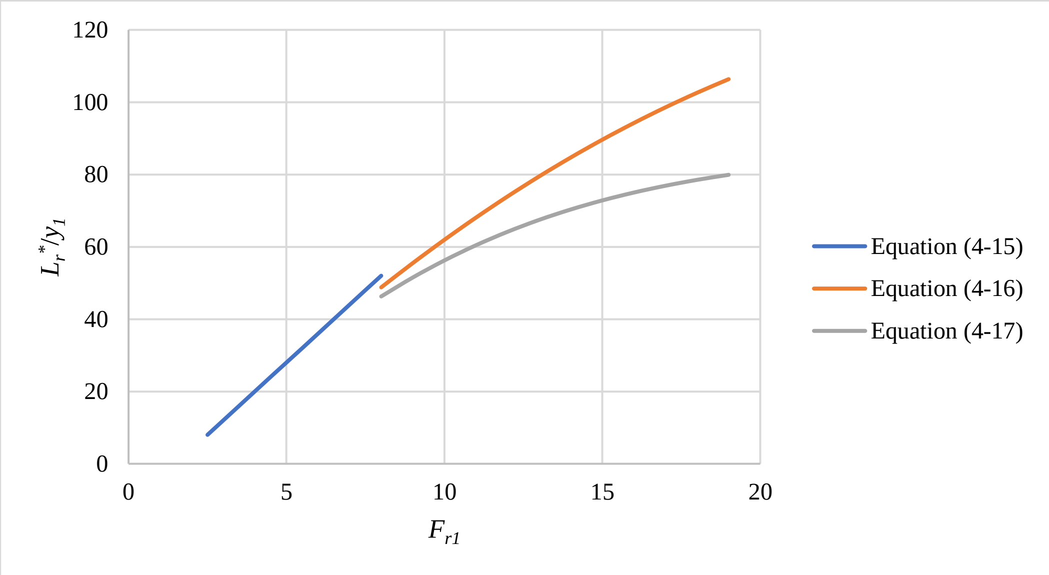

Figure 4-1- Graphical representation of Equations (4-15) to (4-17)

4.1.2.5. Relationship 5 – Alternate method using sequent depth ratio and Froude number

The fifth and final relationship developed differed from the previous four. This relationship only used 30% of the B-jump data from the experiments. Unlike the 50% used previously, the 30% used were not random. Groups of data with the same incoming Froude number (F_{r1}) were chosen. The groups of F_{r1} ranged from 4.10 to 7.77. X/h was plotted against y_3/y_1 in Fig. 4-2

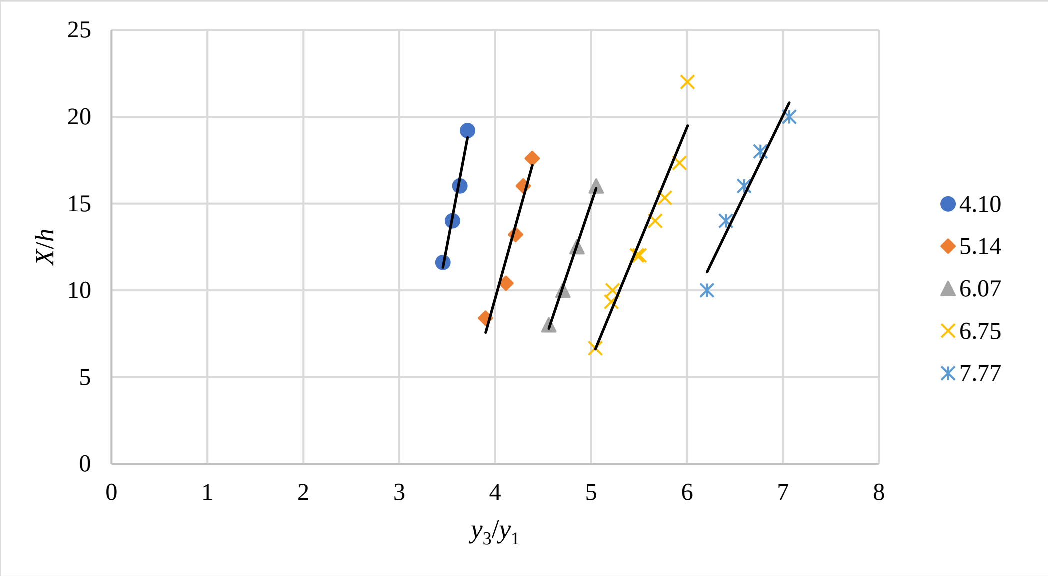

Figure 4-2- X/h for given sequent depth (y_3/y_1) per incoming Froude number (F_{r1})

From Fig. 4-1, linear trendlines were fitted to each Froude number group. The resulting lines of best-fit are presented in Table 4-1 below with their respective correlation coefficients (R^2).

Table 4-1- Line of best-fit equations from Fig. 4-1 and their respective R^2 values

Froude number, F_{r1}	Linear trendline equations	R^2
4.10	$\frac{X}{h} = 29.1\left(\frac{y_3}{y_1}\right) - 89.1$	0.984
5.14	$\frac{X}{h} = 19.8\left(\frac{y_3}{y_1}\right) - 69.7$	0.939
6.07	$\frac{X}{h} = 16.4\left(\frac{y_3}{y_1}\right) - 66.8$	0.997
6.75	$\frac{X}{h} = 13.4\left(\frac{y_3}{y_1}\right) - 60.9$	0.935
7.77	$\frac{X}{h} = 11.4\left(\frac{y_3}{y_1}\right) - 59.6$	0.951

From the linear trendlines in Table 4-1, the gradients correlate with their respective Froude numbers. The gradients (m) are then plotted against F_{r1} and presented in Fig. 4-3.

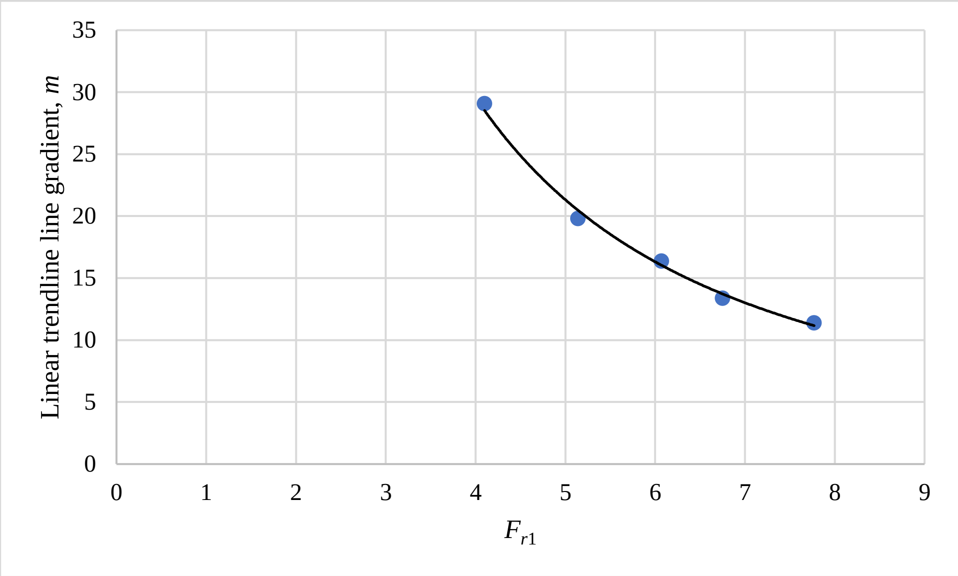

Figure 4-3- The gradients (m) from the best-fit equations in Table 4-1 plotted against F_{r1}

The resulting power trendline is:

$$m = 226{F_{r1}}^{-1.47} \tag{4-18}$$

The correlation coefficient (R^2) for Equation (4-18) is 0.995.

The absolute values of the y-axis intercepts (C) from the linear trendlines in Table 4-1 are also plotted against F_{r1} in Fig. 4-4 below.

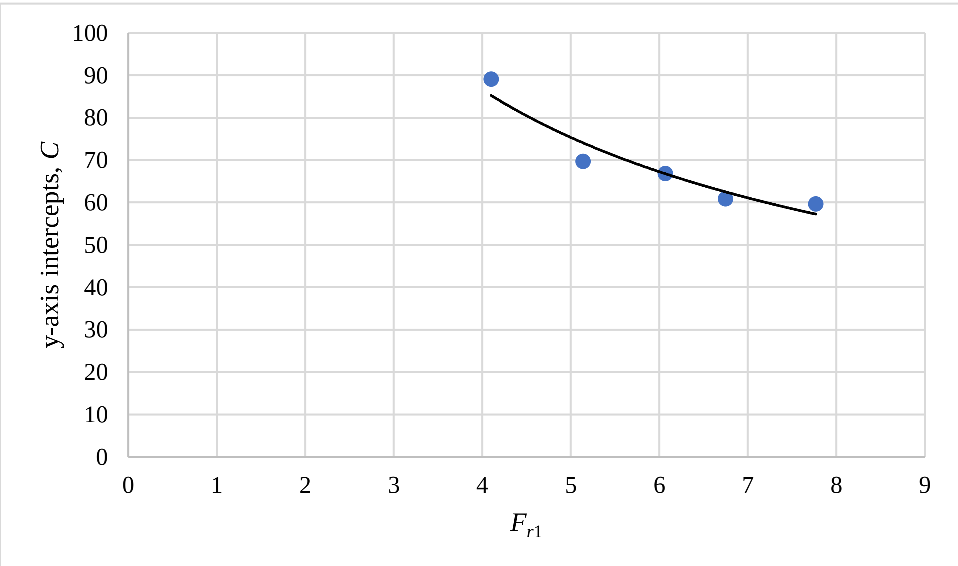

Figure 4-4- The y-axis intercepts from the best-fit equations in Table 4-1 plotted against F_{r1}

The resulting power trendline is:

$$C = 205{F_{r1}}^{-0.623} \tag{4-19}$$

The correlation coefficient (R^2) for Equation (4-19) is 0.923.

The fifth relationship was then produced using the form of a basic linear equation, where *m* and *C* are from Equations (4-18) and (4-19) respectively:

$$\frac{X}{h} = (m)\left(\frac{y_3}{y_1}\right) - C \tag{4-20}$$

4.1.3. Discussion

The research conducted explored the importance of the distance between the hydraulic jump's toe and the abrupt step in the design of an abrupt step stilling basin. From the results, five relationships were developed, each with factors necessary for the design. For relationships 1 to 4, 50% of the experimental results were kept clean for confirmation. The experimental *X*/*h* values were compared with the predicted *X*/*h* values from the relationships. These comparisons are presented below in Fig. 4-5 to 4-9.

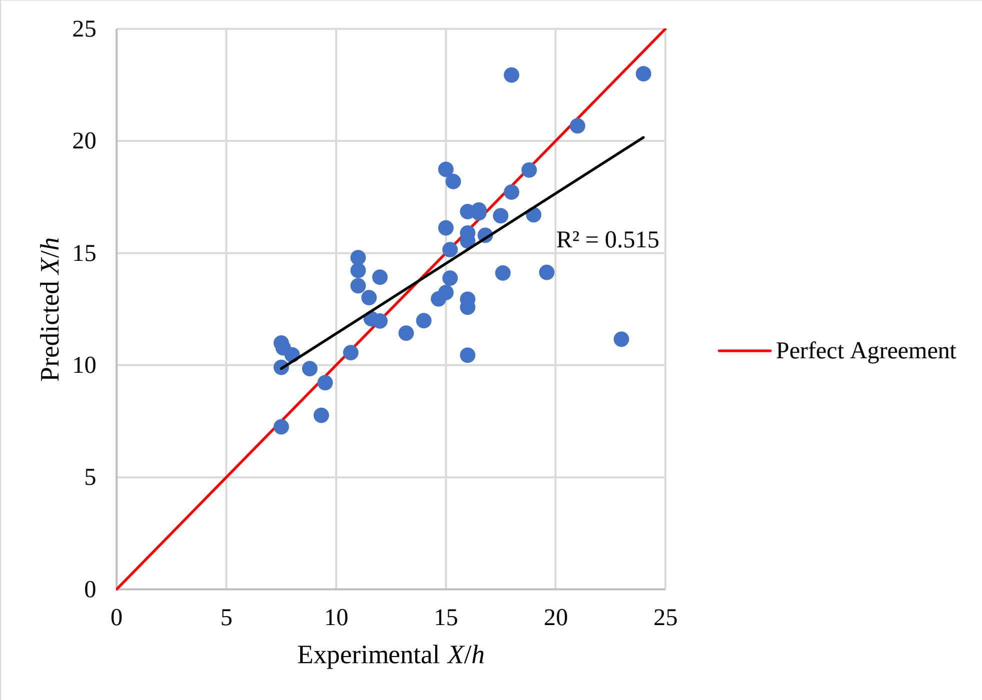

Figure 4-5- Comparison between relationship 1 (Equation (4-3)) and the clean experimental data

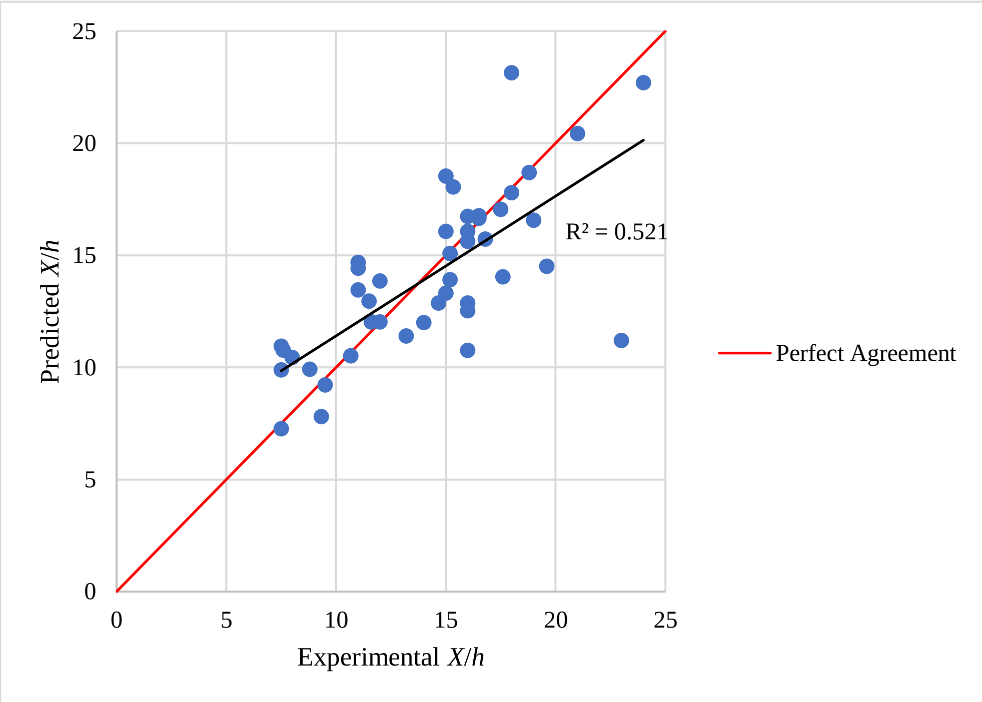

Figure 4-6- Comparison between relationship 2 (Equation (4-6)) and the clean experimental data

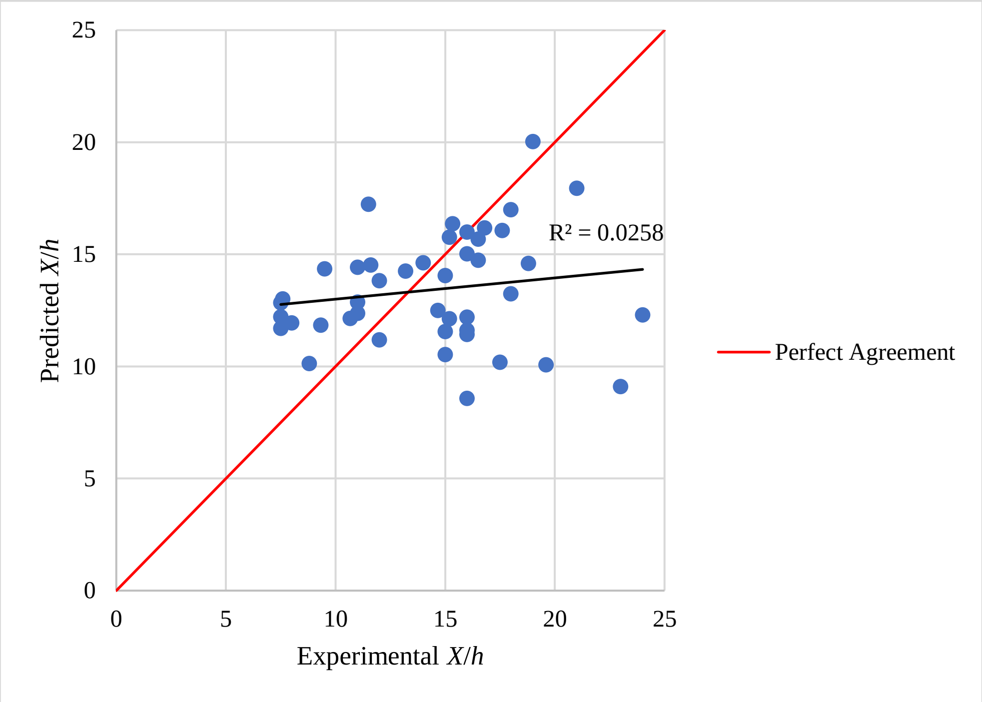

Figure 4-8- Comparison between relationship 3 (Equation (4-11)) and the clean experimental data

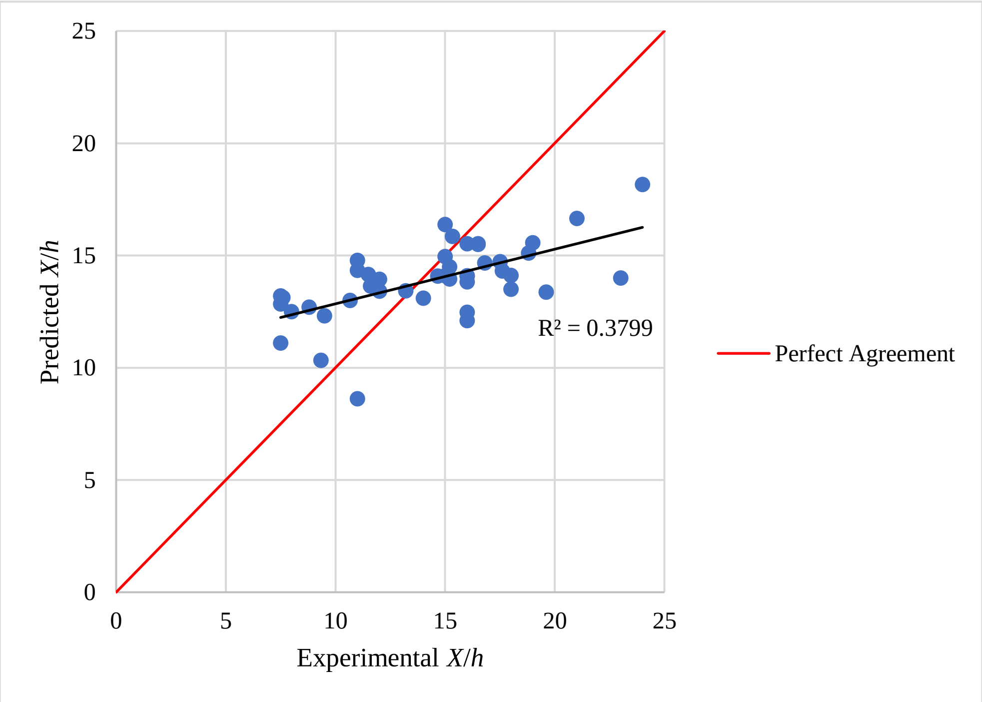

Figure 4-7-Comparison between relationship 4 (Equation (4-14)) and the clean experimental data

In relationship 5, only 30% of the experimental data were used in developing the relationship. Therefore, the other 70% were used when comparing the predicted and experimental *X/h* and presented in Fig. 4-9.

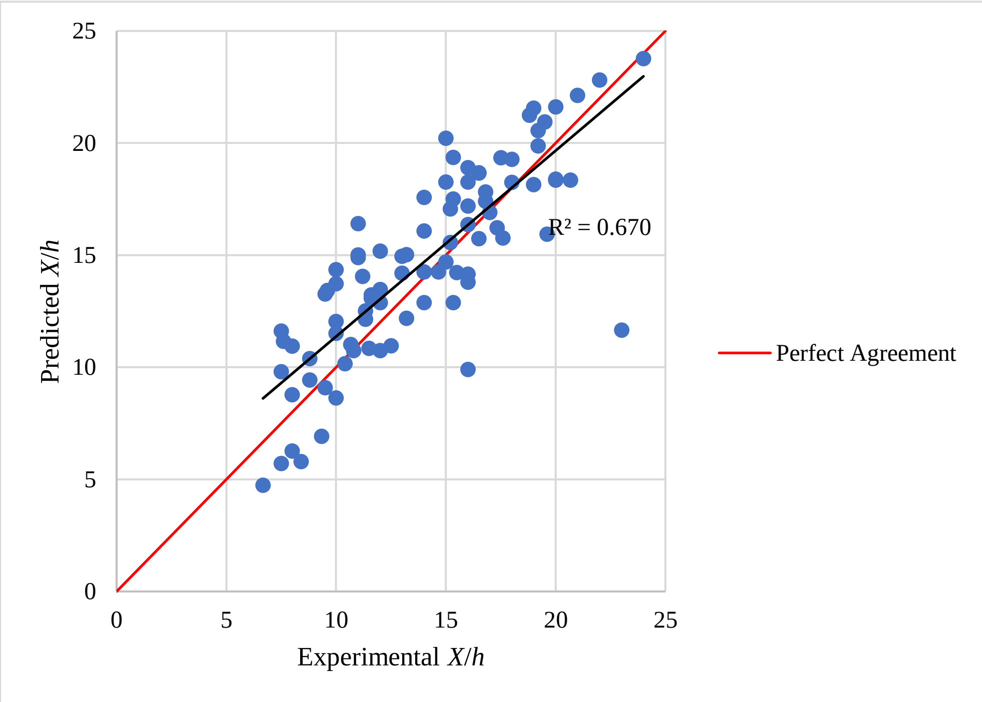

Figure 4-9- Comparison between relationship 5 (Equation (4-20)) and the clean experimental data

The average absolute errors between the measured and the predicted results are presented in Table 4-2 below.

Table 4-2- Relationships 1 to 5 average absolute percentage error when compared with the clean data

Relationship	**Average absolute error (%)**	**Equation**
1	15.1	(4-3)
2	14.9	(4-6)
3	25.2	(4-11)
4	22.2	(4-14)
5	17.1	(4-20)

All five relationships had scatter around the prefect agreement lines. The greatest scatter occurred in relationship 3 (Equation (4-11)). The corresponding R^2 value for the predicted versus measured results was 0.026, showing very poor correlation. The average absolute error for relationship 3 was also the highest at 25.2%. Fig. 4-7 shows the results of relationship 4 (Equation (4-14)). The trend between the predicted and measured results was poor as well with an average absolute error of 22.2%.

Relationships 1, 2, and 5 were the best performing when comparing predicted X/h versus the clean measured X/h. All the average absolute errors were below 20.0%. All the R^2 values were above 0.5, which is not ideal, but the data showed a positive trend with the line of perfect agreement.

All five relationships were compared with results from the study conducted by Hager and Bretz (1986). As type B hydraulic jumps were the focus in the development of the relationships, Forster and Skrinde's (1950) data were not compared as they did not meet the requirements for B-jumps set out in Section 1.1.1. Hager and Bretz (1986) did not measure the distance X explicitly, but the researchers measured the jump's roller length (L_r) and positioned the toe of the jump about $L_r/2$ away from the step. All five relationships predicted X very poorly when compared with the $L_r/2$ from Hager and Bretz's (1986) study. This outcome is not a true representation of the accuracy of the relationships developed as the distance X was not Hager and Bretz's (1986) focus. The researchers also stated in their study that accurate measurements of L_r were "impossible" due to violent wave formation and intense turbulence (Hager & Bretz, 1986). They further mention that the precision with which the measurements were taken was ±0.05 m (Hager & Bretz, 1986).

From the comparison between the clean experimental data and the relationships developed, relationships 2 and 5 are the preferred options. However, all five of the relationships performed poorly with the established experimental data from Hager and Bretz (1986). As discussed, the validity of this comparison is questionable as $L_r/2$ was compared with X. The actual measurement of L_r was also uncertain. A further general concern that could account for the error is scaling. The results produced by Hager and Bretz (1986) were conducted in a larger flume than what was used in this study.

A more localised problem may have occurred in the development of Relationship 3 in which the force on the step was explored. Momentum was used to determine the actual force on the step; however, a momentum correction factor may be necessary to accurately determine the force on the step.

4.2. Sweep-out limitation

Sweep-out occurs when the hydraulic jump is pushed out of the stilling basin and the jump happens downstream of the step. Sweep-out is undesired as the fast supercritical flow then passes over the step and can erode the channel bed downstream. For the abrupt step testing, the starting condition before the key measurements were taken was when the hydraulic jump was in sweep-out. An observation was made that as the jump entered the basin from sweep-out, a minimum condition occurred. This minimum condition would allow the determination of certain limits in the design. Using specific design quantities, a sweep-out limit was developed.

4.2.1. Analysis methodology

For the development of this limiting condition, the critical state was as the jump entered the basin i.e. in-between the vertical sluice gate and the step. As the downstream depth (y_3) was the only variable changed, this became known as y_{3min} when the jump first enters the basin. For abrupt steps, y_{3min} was assumed to be the same as when the jump entered the basin and just before it left the basin, based on the findings by Viero and Defina (2017). If they were not assumed to be the same, hysteresis could be occurring. However, this is explored in chapter 5 of this report. Therefore, the minimum sequent depth ratio for the hydraulic jump could be established by dividing y_{3min} by y_1 (the upstream supercritical flow) i.e.$(y_3/y_1)_{min}$.

Therefore, for each abrupt step height tested, the minimum sequent depth ratio was taken for each incoming Froude number (F_{r1}) tested. This means that only 31 data points were used in the development of the sweep-out limit (Appendix B). Due to the low number of data points, the data were not split for later confirmation. However, separate testing was conducted for Section 5 of this report where a portion of the data was used for comparison.

4.2.2. Results

On first observations, the minimum sequent depth ratio $(y_3/y_1)_{min}$ was thought to be dependent on the incoming Froude number (F_{r1}). Therefore $(y_3/y_1)_{min}$ was plotted against F_{r1} and a basic line of best-fit was fitted to the data (Fig. 4-10).

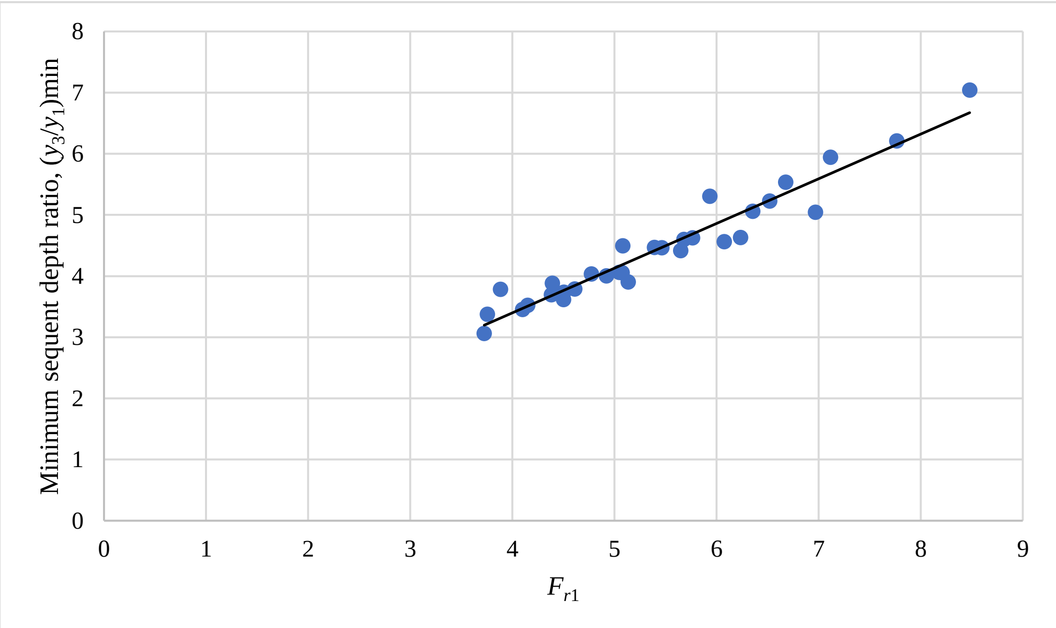

Figure 4-10- Minimum sequent depth ratio ($(y_3/y_1)_{min}$) for incoming Froude numbers (F_{r1})

The line of best-fit produced the following equation

$$\left(\frac{y_3}{y_1}\right)_{min} = 0.731F_{r1} + 0.47 \tag{4-21}$$

The coefficient of determination (R^2) for Equation (4-21) is 0.931.

The practicality of Equation (4-21) came into question as the step height (h) had not been accounted for in the limitation development. Determining the minimum step height that would allow a hydraulic jump to occur in the basin for a given Froude number and sequent depth ratio would be more advantageous in design. A new form of the relationship was then used in which the step height (h) is the subject of the formula. This then gives the minimum h to avoid sweep-out for a given y_3/y_1 and F_{r1}. The step height (h) was then normalised by the incoming flow depth (y_1) and a multiple regression analysis was carried out in the form of:

$$\left(\frac{h}{y_1}\right)_{min} = f\left[\left(\frac{y_3}{y_1}\right)_{min}, F_{r1}\right] \tag{4-22}$$

The resulting multiple regression produced the following relationship:

$$\left(\frac{h}{y_1}\right)_{min} = 0.298\left(\frac{y_3}{y_1}\right)_{min}^{-2.04} {F_{r1}}^{2.66} \tag{4-23}$$

The adjusted correlation coefficient (R^2), accounting for both independent variables, was 0.881.

4.2.3. Discussion

As an additional finding from the previous section, the minimum conditions for a hydraulic jump to occur in the basin were established. These minimum conditions are situational and were determined when the starting position of the hydraulic jump was downstream of the step. It was noticed that the minimum sequent depth ratio that would allow a jump to form in the basin was dependent on the incoming Froude number (Equation (4-21)). However, for this limitation to be practical in design, the step height is needed. Therefore Equation (4-23) was developed in which the minimum step height that will allow a hydraulic jump to occur in the basin can be determined by the sequent depth ratio and the incoming Froude number.

The absolute average error between Equation (4-23) and the data used to develop it was 5.91%. This, however, does not accurately show the strength of the relationship as the data was used in the development of the equation. Fortunately, a portion of the data collected in the next section could be used and the comparisons are made below.

In the next section, two starting conditions are examined. As above, the first starting condition was when the hydraulic jump occurred downstream and moved into the basin. The second was when the hydraulic jump had submerged the vertical sluice gate. The downstream depth was then lowered until the jump swept-out the basin. Both starting conditions were compared with Equation (4-23) and Fig. 4-11 was produced.

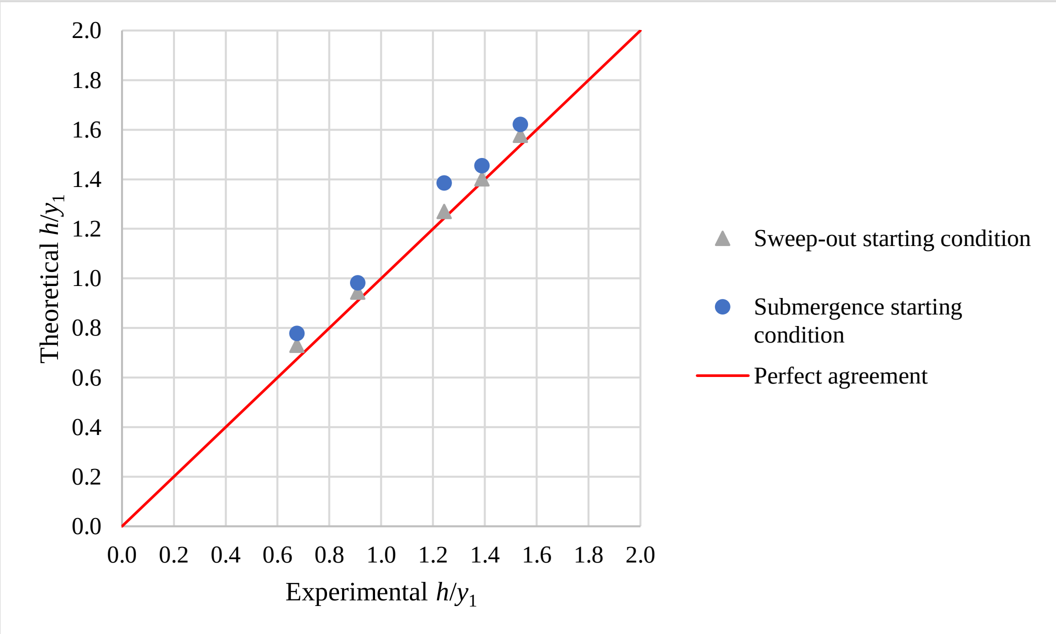

Figure 4-11- Comparison between Equation (4-23) and the clean experimental data

Equation (4-23) compared extremely well with the data that started in sweep-out. The absolute average error was 3.58%. Equation (4-23) overestimated h/y_1 for the submergence starting condition. The absolute average error was 9.02%. This implies a degree of hysteresis occurs for an abrupt step and is dependent on the starting condition of the hydraulic jump. This is further investigated in the next section.

Although Equation (4-23) performs well, its practicality comes into question. The relationship was produced using data that started in sweep-out. However, sweep-out should be avoided in general as the supercritical flow it produces over the step and downstream can have undesirable erosive effects on the channel.

4.3. Practical example

Using relationship 2 (Equation (4-6)), a practical design problem was solved. An upstream flow depth (y_1) of 0.90 m is released from an outlet source at 75 $m^3/s/m$. The downstream flow depth (y_3) is 3.50 m. The width of the channel is 5.0 m. Equation (4-6) requires the incoming Froude number (F_{r1}) and Y_{corr} to determine the design quantity X/h.

The incoming Froude number was calculated using Equation (2-5):

$$F_{r1} = \frac{V}{\sqrt{gy}} \tag{2-5}$$

The resulting Froude number was 5.61.

To determine Y_{corr}, the theoretical sequent depth ratio (y_3^*/y_1) must be calculated for a simple hydraulic jump using the incoming flow conditions. Equation (2-4) was used.

$$\frac{y_3}{y_1} = \frac{1}{2}\left(\sqrt{1 + 8{F_{r1}}^2} - 1\right) \tag{2-4}$$

$y_3{}^*/y_1$ was calculated as 7.44.

Finally using Equation (4-6), X/h was calculated as 4.93.

$$\frac{X}{h} = 47.3(Y_{corr})^{5.13}(F_{r1})^{0.623} \tag{4-6}$$

Using the sweep-out limit in Equation (4-23), the minimum step height (h_{min}) was calculated.

$$\left(\frac{h}{y_1}\right)_{min} = 0.298\left(\frac{y_3}{y_1}\right)_{min}^{-2.04} {F_{r1}}^{2.66} \tag{4-23}$$

The minimum step height was 1.66 m, which means that a step height less than 1.66 m has the potential for the hydraulic jump to sweep-out the basin. The minimum step height would result in the smallest basin of 8.18 m. In practice, a safety factor would need to be applied as the possibility of sweep-out is great.

If the shortest basin length was not the requirement, several designs can be chosen depending if the step height or basin length is the design constraint. If the step height had to be a specific height, the available jump positions are demonstrated in Table 4-3.

Table 4-3- Plausible jump positions away from the step for given step heights

h (m)	2.00	2.25	2.50	2.75	3.00	3.25	3.50
X (m)	9.90	11.1	12.3	13.5	14.8	16.0	17.2

If the basin length had to be a specific size, the position of the jump must be exact. With this criterion, the available design options are presented in Table 4-4.

Table 4-4- Possible step heights for given jump positions

X (m)	10.0	15.0	20.0	25.0	30.0	35.0	40.0
h (m)	2.03	3.04	4.06	5.07	6.09	7.10	8.12

From the above results in Tables 4-3 and 4-4, a step height of 2.00 m would ensure no sweep-out and require a basin length of about 10.0 m. Larger step sizes would be safer but, would also require longer basins.

5. Hysteresis experiment analysis

Hysteresis happens when two stable states occur for the same flow conditions and the governing factor for which state occurs is the history of the flow. This has important implications as fluctuations in the flow may cause its state to change. For it to return to the original flow state, additional flow manipulation may be required and depend on the history of the flow. Alternatively, hysteresis occurs when the hydraulic jump is close to the step (Viero & Defina, 2017). If a short basin design is required, hysteretic conditions may be needed in the design.

This investigation into hysteresis examines the applicability of established hysteresis equations by Viero and Defina (2017). It also investigates the effect of step slope, as well as the effect on hydraulic jump length characteristics. The investigation was conducted using the 10 mm step height. Four slopes and the abrupt step were tested. The slopes tested were 1-in-1, 1-in-2, 1-in-3 and 1-in-4.

5.1. Analysis methodology

The analysis for the hysteresis testing was straightforward. For each test run, an incoming Froude number (F_{r1}) was set by adjusting the incoming flow depth (y_1) and the discharge. The hydraulic jump began in the sweep-out position downstream. The tailwater weir was raised, thus causing the downstream subcritical flow depth (y_3) to increase and moving the jump upstream toward the step. Just as the jump entered the basin, y_3 was measured. This was the lower boundary of the hysteresis region as it was the limit before supercritical to subcritical transition upstream of the step (Appendix C). The position of the jump relative to the step was also measured (X). This was the first significant reading taken. y_3 was then further increased with measurements taken incrementally until it submerged the vertical sluice gate. The reverse was then carried out – y_3 was incrementally decreased causing the jump to move downstream toward the step. Just as the hydraulic jump exited the basin, the subcritical y_3 was measured and this became the second significant reading. This was the upper boundary of the hysteresis region and was the limit before supercritical to subcritical transition downstream (Appendix D). For each step set-up, several incoming Froude numbers (F_{r1}) were tested varying from 4 to 11.

5.2. Results

For each step set-up, the sequent depth (y_3/y_1) was plotted against the incoming Froude number (F_{r1}). This differs from Viero and Defina's (2017) presentation of hysteresis as F_{r1} changed for given h/y_1, whereas Viero and Defina (2017) had a constant F_{r1} for multiple h/y_1. The results are presented in Fig. 5-1 to 5-5 for each step slope.

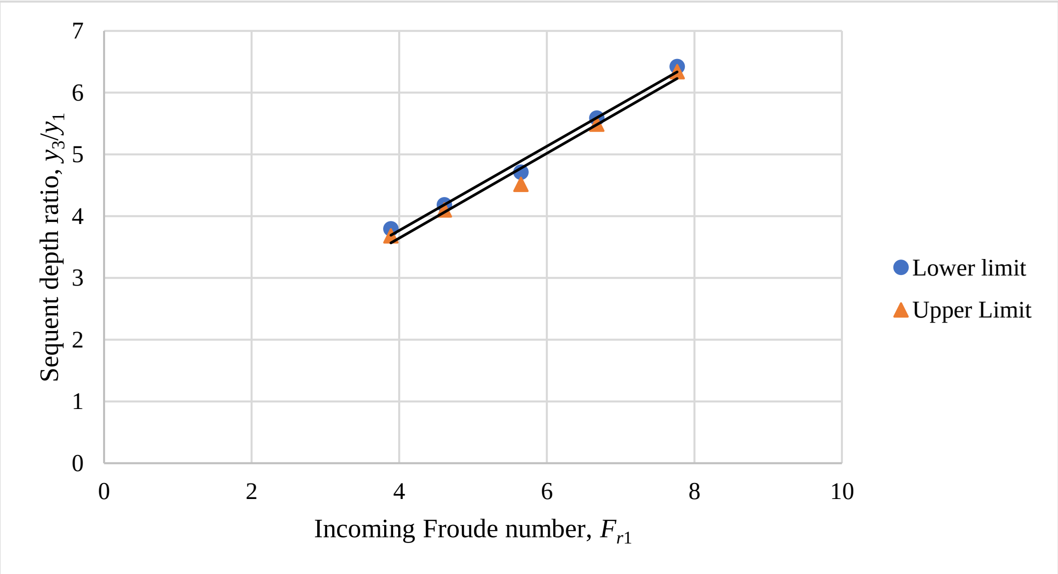

Figure 5-1- Effect of hysteresis on sequent depth ratio (y_3/y_1) and Froude number (F_{r1}) for the 1-in-1 step

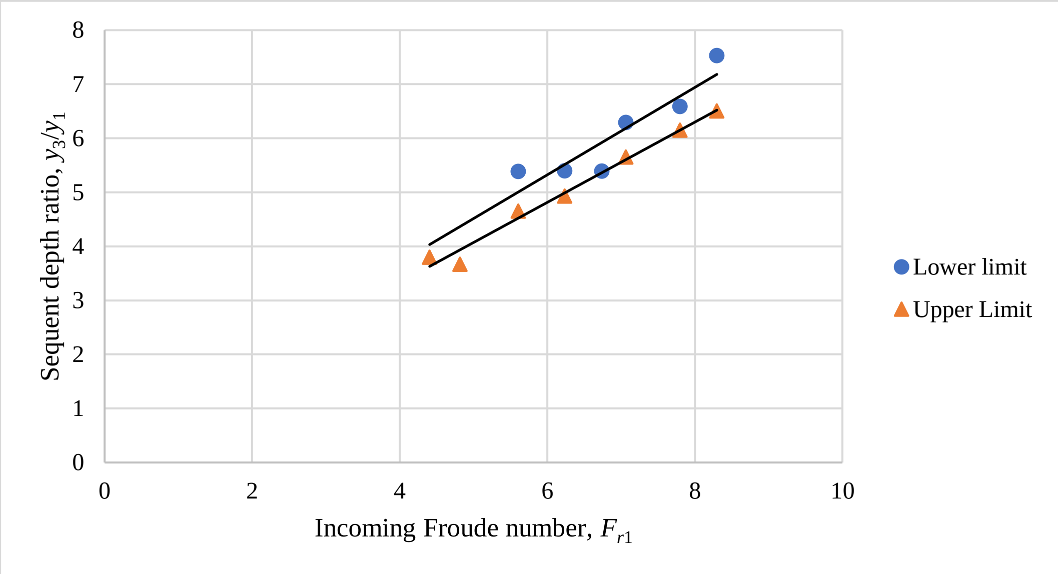

Figure 5-2- Effect of hysteresis on sequent depth ratio (y_3/y_1) and Froude number (F_{r1}) for the abrupt step

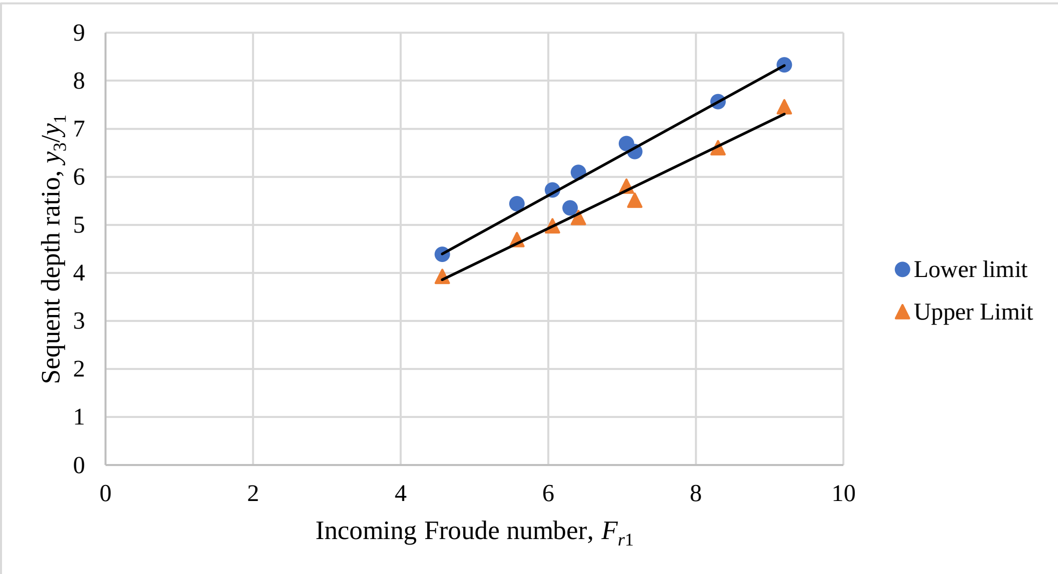

Figure 5-3- Effect of hysteresis on sequent depth ratio (y_3/y_1) and Froude number (F_{r1}) for the 1-in-2 step

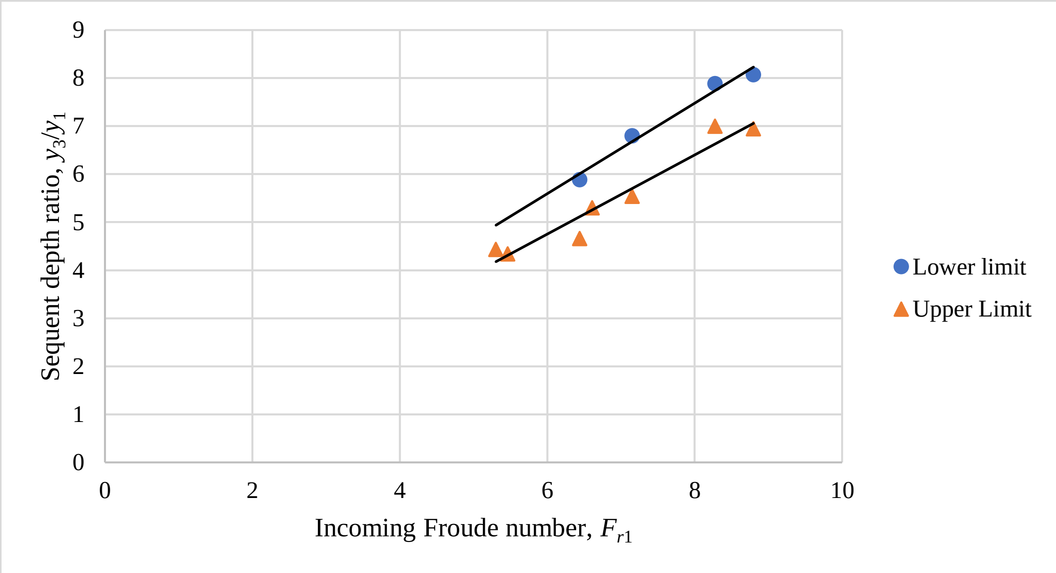

Figure 5-4- Effect of hysteresis on sequent depth ratio (y_3/y_1) and Froude number (F_{r1}) for the 1-in-3 step

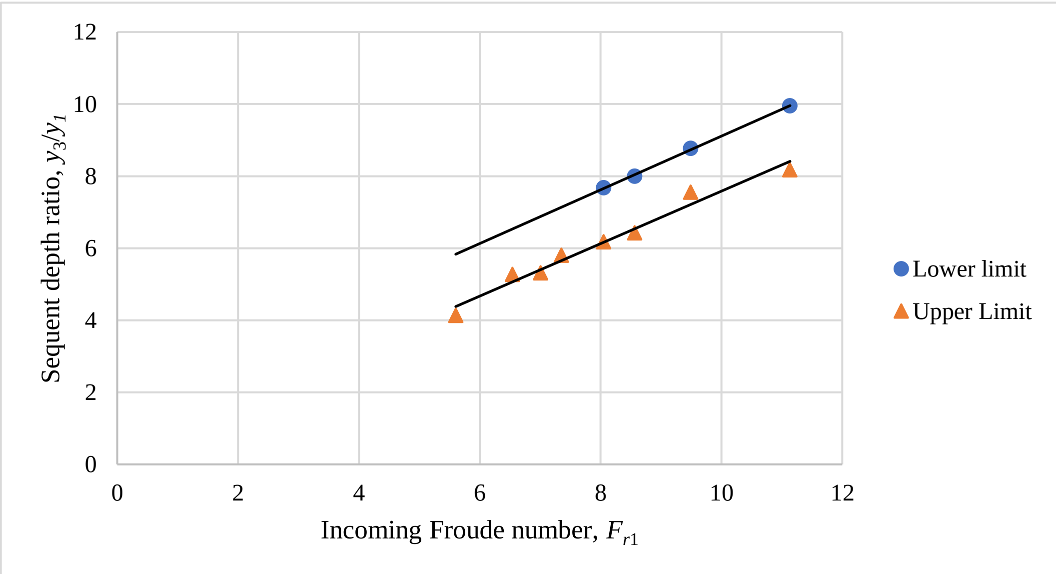

Figure 5-5- Effect of hysteresis on sequent depth ratio (y_3/y_1) and Froude number (F_{r1}) for the 1-in-4step

The resulting lines of best-fit and corresponding coefficient of determination (R^2) from each step slope are presented in Table 5-1 below.

Table 5-1- Equations of the lines of best-fit and R^2 for both lower and upper boundary limits for each step

Step	**Lower Boundary**		**Upper Boundary**	
	Best-fit Equation	$\mathbf{R^2}$	**Best-fit Equation**	$\mathbf{R^2}$
Abrupt	$\frac{y_3}{y_1} = 0.682F_{r1} + 1.04$	0.989	$\frac{y_3}{y_1} = 0.686F_{r1} + 0.999$	0.980
1-in-1	$\frac{y_3}{y_1} = 0.809F_{r1} + 0.469$	0.841	$\frac{y_3}{y_1} = 0.743F_{r1} + 0.357$	0.983
1-in-2	$\frac{y_3}{y_1} = 0.846F_{r1} + 0.533$	0.969	$\frac{y_3}{y_1} = 0.745F_{r1} + 0.463$	0.985
1-in-3	$\frac{y_3}{y_1} = 0.942F_{r1} - 0.0615$	0.976	$\frac{y_3}{y_1} = 0.824F_{r1} - 0.940$	0.940
1-in-4	$\frac{y_3}{y_1} = 0.745F_{r1} + 1.66$	0.999	$\frac{y_3}{y_1} = 0.728F_{r1} + 0.300$	0.973

The y_3/y_1 versus F_{r1} relationship showed a very consistent trend for each step set-up. The average R^2 value for the trendlines in each graph for each set-up was 0.963, with a range of 0.841 to 0.999.

Following on from the sequent depth ratio relationships above, it was observed that as the jump entered the basin from sweep-out (lower limit), it occurred at a certain distance away from the step. This distance was observed to depend on the incoming

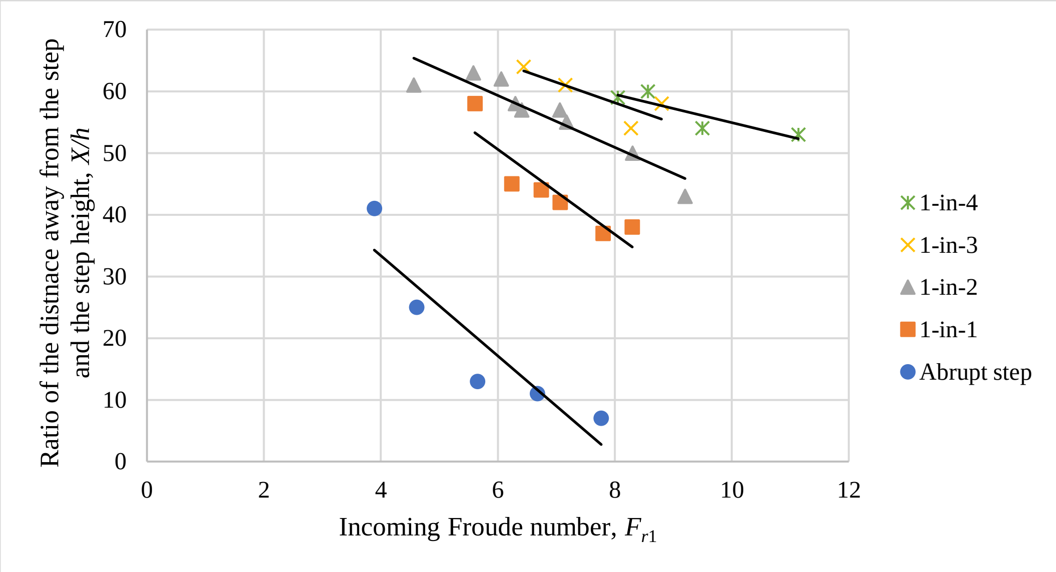

Figure 5-6- Lower limit correlations between X/h and F_{r1}

Froude number (F_{r1}). The distance was then normalised against the step height (h) and plotted against F_{r1}. The results from each step height are presented in Fig. 5-6.

The lines of best-fit from Fig. 5-6 above and their respective coefficient of determination (R^2) are presented in Table 5-2.

Table 5-2- Resulting lines of best-fit and their R^2 values for each step from Fig. 5-6

Step set-up	**Line of best-fit**	**R^2**
Abrupt	$\frac{X}{h} = -8.12F_{r1} + 65.8$	0.838
1-in-1	$\frac{X}{h} = -6.88F_{r1} + 91.9$	0.813
1-in-2	$\frac{X}{h} = -4.20F_{r1} + 84.6$	0.861
1-in-3	$\frac{X}{h} = -3.32F_{r1} + 84.7$	0.686
1-in-4	$\frac{X}{h} = -2.29F_{r1} + 77.8$	0.779

As carried out above for the lower limit, the upper limit X/h versus Fr_1 was plotted. The results from each step height are presented in Fig.5-7

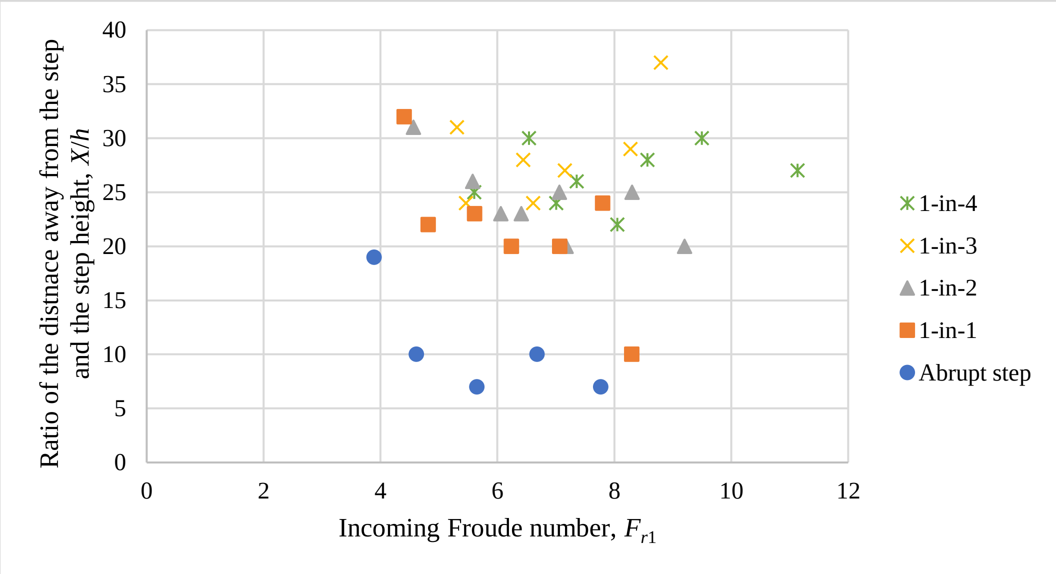

Figure 5-7- Upper limit correlations between X/h and F_{r1}

The correlation between *X*/*h* and Fr_1 was very poor for the upper limit, therefore no trendlines were fitted to the results. However for the abrupt step, a trend was observed and both the upper and lower limits of *X*/*h* versus F_{r1} were plotted in Fig. 5-8.

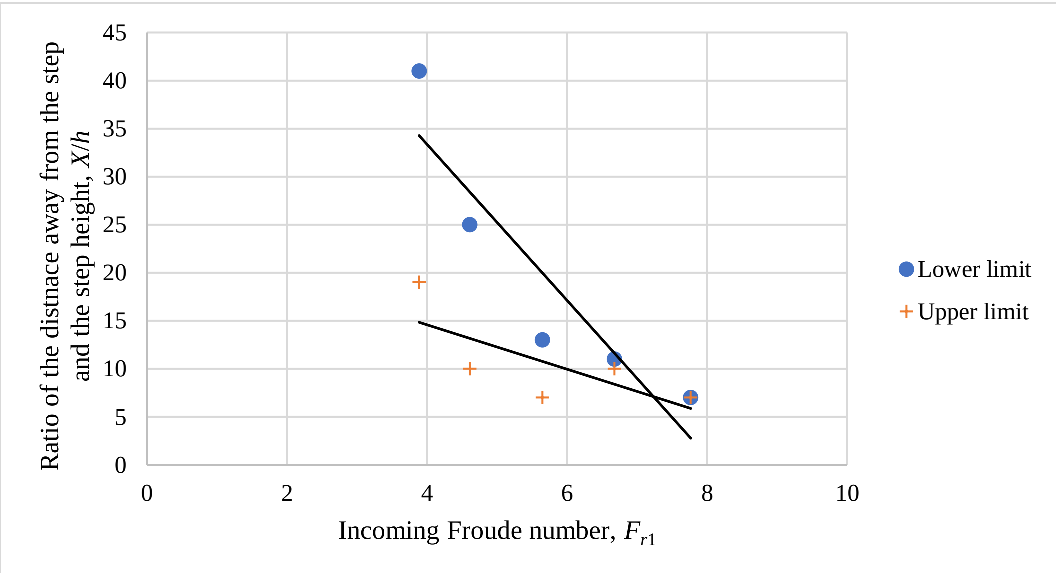

Figure 5-8- Lower and upper limit correlations between X/h and F_{r1} for the abrupt step

The lines of best-fit from Fig. 5-8 above and their respective coefficients of determination (R^2) are presented in Table 5-3.

Table 5-3- Abrupt step lower and upper limit lines of best-fit and R^2 from Fig. 5-8

Limit	Line of best-fit	R^2
Lower	$\frac{X}{h} = -8.12F_{r1} + 65.8$	0.838
Upper	$\frac{X}{h} = -2.31F_{r1} + 23.8$	0.533

5.3. Discussion

In Fig. 5-1 to 5-5, the experimental sequent depth ratio (y_3/y_1) was plotted against the incoming Froude number (Fr_1) for both lower and upper limits. For the abrupt step (Fig. 5-1), the gap between the lower and upper limit is very small. This gap is the hysteretic region. This was expected, as Viero and Defina (2017) explained in their study, and is due to the greater amount of energy dissipation through the abrupt step. As the sloping steps are introduced (Fig. 5-2 to 5-5), a clear gap develops between the limits. Furthermore, as the slope of the step becomes more gradual, the gap between the limits increases. This was again anticipated by Viero and Defina (2017) as the energy dissipation through the step decreases for shallow step slopes.

The practicality of sloping steps is an issue. Firstly, the primary goal of using steps in a stilling basin is to dissipate energy, therefore sloping steps would not be the most effective solution. Secondly, as the results above have shown, the reliability of sloping steps is poor due to the hysteretic region. Abrupt steps are and have been favoured for these reasons. However under certain conditions, sloping steps could be used and this is explained later in the section.

The experimental data from all the steps were then compared with the established theoretical relationships by Viero and Defina (2017). The researchers showed their relationships in terms of h/y_1 vs F_{r1} or F_{r3}. However, this was found not to be the best method to compare this study's experimental data with their relationships. No single F_{r1} was chosen for multiple h/y_1 in the investigation. As such, Viero and

Defina's (2017) relationships were rearranged to produce the theoretical y_3 and therefore, the theoretical sequent depth ratio (y_3/y_1) for the theoretical upper and lower limits of the hysteresis region.

Using the lower boundary limit developed by Viero and Defina (2017) (Equation (2-21)), the sequent depth ratio at the lower boundary can be calculated.

$$E_1 \geq E_3^* + (E_{loss} + h) \tag{2-21}$$

The flow depth y_1 was known, therefore E_1 could be calculated. E_{loss} and h are the energy losses due to the energy dissipation and the step, respectively. The theoretical energy dissipated through the step was unknown, but the step height (h) was known. Therefore, the energy losses (E_{loss} and h) were assumed to just be h. E_3^* could then be calculated using Equation (2-21), which meant y_3^* was known. y_3^* was the supercritical flow depth after the step when the jump was downstream of the step. Using momentum conservation downstream of the step through the hydraulic jump, the theoretical subcritical flow depth downstream (y_3) could then also be calculated. Dividing y_3 by y_1 gave the theoretical sequent depth ratio for the lower limit.

Using Equation (2-23), determining the sequent depth ratio for the upper limit followed the same procedure.

$$E_1 \leq E_2^* \tag{2-23}$$

For clarity, section 2 was located just in front of the step when the hydraulic jump had entered the basin. Using momentum conservation through the hydraulic jump upstream of the step (between section 1 and 2), the subcritical flow depth in front of the step was determined (y_2^*). As subcritical flow occurs over the step, the specific energy at section 2 is equal to the specific energy downstream at section 3 plus the step height (h).

$$E_2 = E_3 + h \tag{5-1}$$

E_3 was then calculated, therefore the theoretical y_3 was determined. Dividing y_3 by y_1 gave the theoretical sequent depth ratio for the upper limit.

In Fig. 5-9, the theoretical sequent depths were compared with the sequent depths from the experiments for both upper and lower limits.

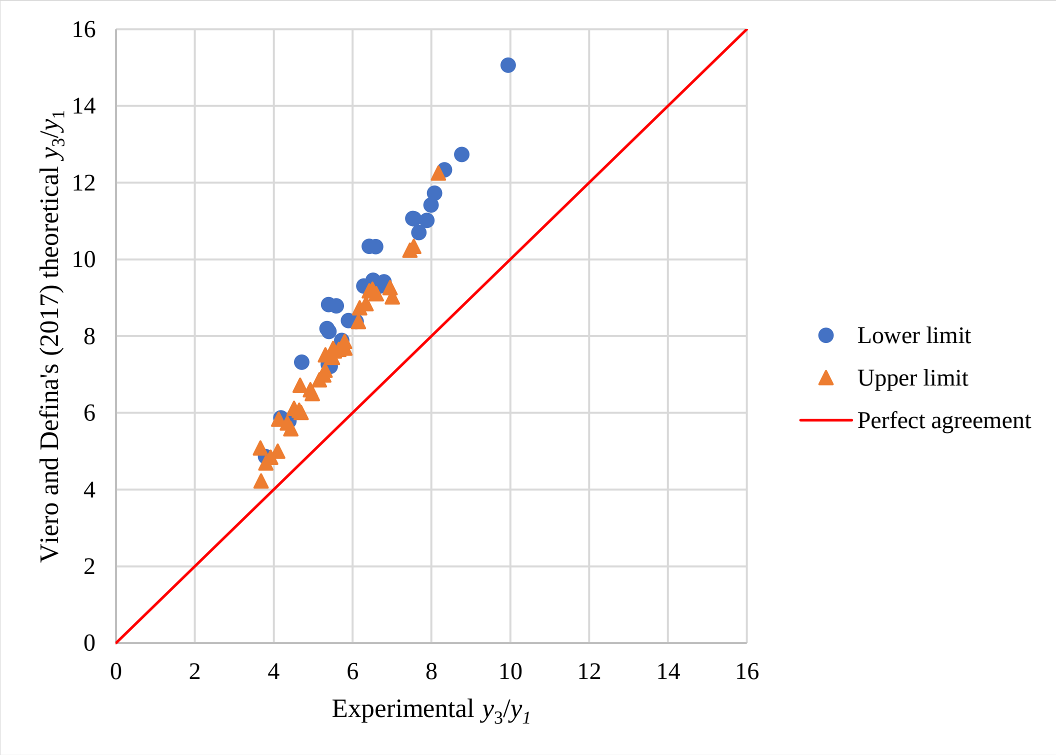

Figure 5-9- Sequent depth ratio comparison between Viero and Defina's (2017) theoretical results and the experimental results for both lower and upper limits of all the steps

The upper limit had an average percentage error of 29.2%. Interestingly, the theoretical results were an average of 1.37 times bigger than the experimental results, with a standard deviation on 0.0872. The lower limits had an average percentage error of 30.3%, but the theoretical results were an average of 1.42 times bigger than the experimental results, with a standard deviation on 0.0994. The low standard deviation (> 0.1) for both limits showed the errors between the theoretical and experimental results had very consistent magnitudes.

There appears to be an inherent error between the experimental data and the theoretical results. Accounting for the loss of energy through the step in the theoretical calculations would cause the hysteresis region to shrink according to Viero and Defina (2017), but not shift both limits. However a range of approximated energy dissipation terms were incorporated into the theoretical calculations, which caused the theoretical calculations to shift towards the experimental results. The magnitude of the error between the theoretical and the experimental was not constant when only energy dissipation was under observation. The slope of the step did not influence the amount of energy dissipated. The energy dissipation required to shift the theoretical results was greater for higher incoming Froude numbers and higher sequent depth ratios, regardless of the step slope. Another factor could be the need to account for energy and momentum correction factors. A range of energy and momentum factors were used to correct the errors, however, only when the factors were less than 1 did the results start to correlate. Energy and momentum factors less than 1 are not common in literature and in practice. However, a combination of accounting for energy dissipation through the step, and incorporating energy and momentum correction factors could bring the theoretical results closer to the experimental results. Further investigation is therefore required to predict the expected energy loss through a step and appropriate utilisation of energy and momentum correction factors. A final possible explanation for the error could be the effect of scaling in the experiments.

In Viero and Defina's (2017) study, the researchers stated that if the F_{r1} was kept constant and the F_{r3} was changed, the jump would not be able to leave the basin above a certain h/y_1 if it started in submergence (Fig. 2-1). This was observed in this study's experimental results, but not at the same theoretical limits calculated by Viero and Defina (2017). This could be as a result of the discrepancy between the theoretical and experimental results above. This would allow the use of sloping steps as effective energy dissipating structures. It would not apply to abrupt steps as there would need to be a distinct hysteresis region. If the hysteresis region can then be accurately predicted starting from submergence, a hydraulic jump would not be able to sweep-out of a basin if the flow conditions mentioned are satisfied.

This would be useful if the energy dissipation required is small, but still needs to occur reliably.

The second set of results dealt with the effect of hysteresis on the position of the jump in the basin. For Fig. 5-6, it was observed that starting from sweep-out, as the jump enters the basin, the jump position varies according to F_{r1}. As F_{r1} increases, the jump occurs closer to the step as it enters the basin. Following that, the degree to which F_{r1} influences the position of the jump as it enters the basin lessens as the slope of the step becomes flatter. This is evident from Table 5-2, in which the gradients of the trendlines become less steep, going from the abrupt step to the 1-in-4 sloping step. This could be explained by the amount of energy dissipated at the step and the energy of the incoming flow. The higher the energy of the incoming flow, the more resistance it can provide against the increase in energy from the increase in y_3 downstream. Furthermore, the energy lost through the step was not as great for the sloping step as it was for the abrupt step. Therefore as the jump enters the basin, the energy of the incoming flow has a lesser effect.

Fig. 5-7 shows the results for X/h versus F_{r1} when the hydraulic jump started from submergence (upper limit). It is evident that there exists no discernible trend between the two characteristics. The results for the abrupt step are noticeably different from the sloping steps and this is discussed below. However for the sloping steps, the average X/h value before the jump sweep-out the basin was 25.2. Fig.5-7 only shows the results of the jumps that were able to sweep-out. As mentioned, if the F_{r1} was great enough for a sloping step, the jump would not be able to sweep-out. However, not enough data were produced from those experimental runs as the focus during the investigation was to replicate hysteresis.

Finally, Viero and Defina (2017) state that if the step is abrupt and h/y_1 is plotted against F_{r1} or F_{r3}, the hysteresis region collapses into a single boundary. This was confirmed by Fig. 5-1 for y_3/y_1 versus F_{r1} from the experiments. However, hysteresis has a greater effect on the distance of the jump from the step. From Fig. 5-8, there was a distinct region between the distance of the jump when it first enters the basin from sweep-out and just before it exits the basin from submergence. Two lines of best-fit were fitted, which could be proposed as limits to the hysteresis zone. Unfortunately, only a small amount of data was available to develop these relationships and therefore, definitive limits cannot be proposed. Further research is required to investigate these potential limits, with the need for a greater data set and varying step heights.

6. Conclusion and recommendations

This investigation was broken down into three sections. The first section explored the relationship between the location of B-jumps and the step height and sequent depth ratio. Five equations (Equations (4-3), (4-6), (4-11), (4-14), and (4-20)) were developed from experimental data to describe this relationship and have been confirmed with independent data.

The next section developed a limiting condition (Equation (4-23)) for abrupt steps to prevent sweep-out of the jump from a basin using experimental data.

Finally, the hysteretic behaviour of a hydraulic jump in association with an upward step was demonstrated. The occurrence of a jump near the step depends on the starting flow conditions. The hysteresis effect is minimal for an abrupt step regarding the sequent depth ratio, however there exists an effect on the distance of the jump from the step at lower Froude numbers.

For the abrupt step design relationships developed, the results were not consistent with other work done by Hager and Bretz (1986). As mentioned in this study, the results cannot be explicitly compared due to inconsistencies between measurements taken. However, further research should be conducted using large-scale experiments and expand on these differences.

Large-scale testing should also be conducted for the hysteresis effect. This could help explain and the inconsistencies between Viero and Defina's (2017) theoretical results. However, an accurate determination of the energy dissipated through the step, and energy and momentum correction factors are also necessary. This could provide useful design information when using a sloping step.

References

Burden, R. L. & Faires, J. D., 2011. *Numerical Analysis.* 9th ed. Boston: Cengage Learning.

Chadwick, A., Morfett, J. & Borthwick, M., 2013. *Hydraulics in Civil and Environmental Engineering.* 5th ed. Boca Raton: CRC Press.

Defina, A. & Susin, F. M., 2006. Multiple states in open channel flow. In: M. Brocchini & F. Trivellato, eds. *Vorticity and Turbulence Effects in Fluid Structure Interaction: An Application to Hydraulic Structure Design.* Southampton: Wessex Insitute of Technology Press, pp. 105-130.

Einwachter, J., 1930. *Wehre und Sohlabstuerze.* 1st ed. Munich and Berlin: Oldenbourg.

Fiuzat, A. A., 1986. Flow characteristics of the hydraulic jump in a stilling basin with an abrupt bottom rise. *Journal of hydraulic research,* 24(3), pp. 207-209.

Forster, J. W. & Skrinde, R. A., 1950. Control of the Hydraulic Jump by Sills. *American Society of Civil Engineers Transactions,* 115(2415), pp. 973-1022.

Hager, W. H., Bremen, R. & Kawagoshi, N., 1990. Classical hydraulic jump; length of roller. *Journal of Hydraulic Research,* 28(5), pp. 591-608.

Hager, W. H. & Bretz, N. V., 1986. Hydraulic jumps at positive and negative steps. *Journal of Hydraulic Research,* 24(4), pp. 237-253.

Hager, W. H. & Li, D., 1992. Sill-controlled energy dissipator. *Journal of Hydraulic Research,* 30(2), pp. 165-181.

Hager, W. H. & Sinniger, R., 1985. Flow characteristics of the hydraulic jump in a stilling basin with an abrupt bottom rise. *Journal of Hydraulic Research,* 23(2), pp. 101-113.

James, C. S., 2018. *CIVN 7016 – Hydraulic Structures Course Notes.* Johannesburg: University of the Witwatersrand.

Karki, K. S. & Mishra, S. K., 1986. Flow characteristics of the hydraulic jump in a stilling basin with an abrupt bottom rise. *Journal of Hydraulic Research,* 24(3), pp. 210-215.

Laushey, L. M., 1950. Control of the hydraulic jump by sills. *American Society of Civil Engineers Transactions,* Volume 115, pp. 996-1002.

Microsoft, 2020. *Use the Analysis ToolPak to perform complex data analysis.* [Online]
Available at: https://support.microsoft.com/en-us/office/use-the-analysis-toolpak-to-perform-complex-data-analysis-6c67ccf0-f4a9-487c-8dec-bdb5a2cefab6
[Accessed 3 August 2020].

Montgomery, D. C. & Runger, G. C., 2011. *Applied Statistics and Probability for Engineers.* 5th ed. New Jersey: John Wiley & Sons.

Muskatirovic, D. & Batinic, D., 1977. *The influence of abrupt change of channel geometry on hydraulic regime characteristics.* Baden-Baden, 17th IAHR-congress, pp. 397-404.

Peterka, A. J., 1983. *Hydraulic design of stilling basins and energy dissipators.* 7th ed. Denver: Engineering Monograph No. 25.

Rajaratnam, N., 1965. The hydraulic jump as wall jet. *Journal of the Hydraulics Division,* 91(HY5), pp. 107-132.

Safranez, K., 1929. Untersuchungen ueber den Wechselsprung. *Der Bauingenieur*, pp. 649-657, 673-678.

Schroder, R., 1957. *Untersuchungen ueber diskontinuierliche Abflussvorgaenge in Freispiegelgerinnen.* Berlin: TU Berlin.

Viero, D. P. & Defina, A., 2017. Extended theory of hydraulic hysteresis in open-channel flow. *Journal of Hydraulic Engineering*, 143(9).

Woycicki, K., 1931. *Wassersprung, Deckwalze und Ausfluss unter einer Schütze.* Warschau: Verlag der polnischen Akademie der technischen Wissenschaften.

Appendix A

Table A-1- Raw experimental data for the abrupt step testing

Step height, *h* (cm)	**Discharge, Q (l/s)**	**y_0 (cm)**	**y_1 (cm)**	**y_3 (cm)**	**X (cm)**
0.500	0.972	7.96	0.801	2.93	11.0
0.500	0.972	7.96	0.801	2.97	24.0
0.500	0.972	7.96	0.801	3.12	30.0
0.500	0.972	7.96	0.801	3.26	42.0
0.500	0.972	7.96	0.801	3.38	53.0
0.500	0.972	7.96	0.801	3.49	66.0
0.500	1.25	11.0	0.902	4.17	27.0
0.500	1.25	11.0	0.902	4.31	34.0
0.500	1.25	11.0	0.902	4.45	46.0
0.500	1.25	11.0	0.902	4.53	54.0
0.500	1.25	11.0	0.902	4.67	61.0
0.500	1.25	11.0	0.902	4.75	66.0
0.500	0.972	10.3	0.701	3.32	20.0
0.500	0.972	10.3	0.701	3.58	40.0
0.500	0.972	10.3	0.701	3.77	52.0
0.500	0.972	10.3	0.701	3.88	66.0
0.500	1.25	12.8	0.813	4.35	22.0
0.500	1.25	12.8	0.813	4.50	30.0
0.500	1.25	12.8	0.813	4.65	40.0
0.500	1.25	12.8	0.813	4.81	52.0
0.500	1.25	12.8	0.813	4.94	61.0
0.500	1.25	12.8	0.813	5.12	66.0
0.500	0.694	11.0	0.500	2.66	16.0
0.500	0.694	11.0	0.500	2.85	28.0
0.500	0.694	11.0	0.500	3.11	37.0
0.500	0.694	11.0	0.500	3.24	50.0
0.500	0.694	11.0	0.500	3.46	66.0
0.500	0.972	15.7	0.561	3.68	17.0
0.500	0.972	15.7	0.561	4.01	27.0
0.500	0.972	15.7	0.561	4.29	42.0
0.500	0.972	15.7	0.561	4.46	51.0
0.500	0.972	15.7	0.561	4.61	60.0
0.500	0.972	15.7	0.561	4.73	66.0
0.500	0.694	15.4	0.409	2.66	11.0

Step height, *h* (cm)	**Discharge, Q (l/s)**	**y_0 (cm)**	**y_1 (cm)**	**y_3 (cm)**	***X* (cm)**
0.500	0.694	15.4	0.409	2.77	18.0
0.500	0.694	15.4	0.409	3.05	26.0
0.500	0.694	15.4	0.409	3.25	37.0
0.500	0.694	15.4	0.409	3.45	48.0
0.500	0.694	15.4	0.409	3.57	55.0
0.500	0.694	15.4	0.409	3.79	66.0
0.500	0.694	20.7	0.355	2.99	10.0
0.500	0.694	20.7	0.355	3.07	25.0
0.500	0.694	20.7	0.355	3.22	33.0
0.500	0.694	20.7	0.355	3.73	40.0
0.500	0.694	20.7	0.355	3.90	48.0
0.500	0.694	20.7	0.355	4.00	55.0
0.500	0.694	20.7	0.355	4.11	66.0
1.00	2.19	13.5	1.48	5.61	34.0
1.00	2.19	13.5	1.48	5.82	43.0
1.00	2.19	13.5	1.48	6.00	53.0
1.00	2.19	13.5	1.48	6.17	61.0
1.00	2.19	13.5	1.48	6.27	66.0
1.00	1.67	12.0	1.10	4.17	23.0
1.00	1.67	12.0	1.10	4.26	31.0
1.00	1.67	12.0	1.10	4.40	38.0
1.00	1.67	12.0	1.10	4.55	47.0
1.00	1.67	12.0	1.10	4.70	58.0
1.00	1.67	12.0	1.10	4.79	66.0
1.00	1.28	13.7	0.805	3.55	8.0
1.00	1.28	13.7	0.805	3.69	23.0
1.00	1.28	13.7	0.805	3.92	32.0
1.00	1.28	13.7	0.805	4.19	42.0
1.00	1.28	13.7	0.805	4.34	53.0
1.00	1.28	13.7	0.805	4.50	63.0
1.00	1.28	13.7	0.805	4.66	66.0
1.00	1.67	17.1	0.930	4.94	15.0
1.00	1.67	17.1	0.930	5.14	24.0
1.00	1.67	17.1	0.930	5.22	35.0
1.00	1.67	17.1	0.930	5.41	49.0
1.00	1.67	17.1	0.930	5.62	59.0
1.00	1.67	17.1	0.930	5.77	66.0
1.00	1.28	16.8	0.720	3.99	13.0

Step height, h (cm)	Discharge, Q (l/s)	y_0 (cm)	y_1 (cm)	y_3 (cm)	X (cm)
1.00	1.28	16.8	0.720	4.13	17.0
1.00	1.28	16.8	0.720	4.44	32.0
1.00	1.28	16.8	0.720	4.61	45.0
1.00	1.28	16.8	0.720	4.85	57.0
1.00	1.28	16.8	0.720	4.96	66.0
1.00	1.28	18.5	0.690	4.10	13.0
1.00	1.28	18.5	0.690	4.29	20.0
1.00	1.28	18.5	0.690	4.49	28.0
1.00	1.28	18.5	0.690	4.60	41.0
1.00	1.28	18.5	0.690	4.76	52.0
1.00	1.28	18.5	0.690	4.83	60.0
1.00	1.28	18.5	0.690	4.95	66.0
1.00	1.28	20.3	0.651	4.04	10.0
1.00	1.28	20.3	0.651	4.17	14.0
1.00	1.28	20.3	0.651	4.29	16.0
1.00	1.28	20.3	0.651	4.40	18.0
1.00	1.28	20.3	0.651	4.60	20.0
1.00	1.28	20.3	0.651	4.75	30.0
1.00	1.28	20.3	0.651	4.96	42.0
1.00	1.28	20.3	0.651	5.17	52.0
1.00	1.28	20.3	0.651	5.34	61.0
1.00	1.28	20.3	0.651	5.44	66.0
1.00	1.28	22.3	0.614	4.32	11.0
1.00	1.28	22.3	0.614	4.49	14.0
1.00	1.28	22.3	0.614	4.60	18.0
1.00	1.28	22.3	0.614	4.74	18.0
1.00	1.28	22.3	0.614	5.16	43.0
1.00	1.28	22.3	0.614	5.38	52.0
1.00	1.28	22.3	0.614	5.48	66.0
1.50	2.39	14.5	1.50	5.28	37.0
1.50	2.39	14.5	1.50	5.50	44.0
1.50	2.39	14.5	1.50	5.73	52.0
1.50	2.39	14.5	1.50	5.82	60.0
1.50	2.39	14.5	1.50	5.94	66.0
1.50	2.53	16.4	1.50	5.83	31.0
1.50	2.53	16.4	1.50	6.09	41.0
1.50	2.53	16.4	1.50	6.23	50.0
1.50	2.53	16.4	1.50	6.35	61.0

Step height, *h* (cm)	**Discharge, Q (l/s)**	**y_0 (cm)**	**y_1 (cm)**	**y_3 (cm)**	**X (cm)**
1.50	2.53	16.4	1.50	6.52	66.0
1.50	2.22	15.3	1.35	5.06	33.0
1.50	2.22	15.3	1.35	5.28	40.0
1.50	2.22	15.3	1.35	5.43	49.0
1.50	2.22	15.3	1.35	5.61	58.0
1.50	2.22	15.3	1.35	5.77	66.0
1.50	2.22	18.5	1.25	5.62	24.0
1.50	2.22	18.5	1.25	5.82	36.0
1.50	2.22	18.5	1.25	6.03	47.0
1.50	2.22	18.5	1.25	6.15	57.0
1.50	2.22	18.5	1.25	6.24	66.0
1.50	1.97	17.9	1.10	4.91	17.0
1.50	1.97	17.9	1.10	5.03	22.0
1.50	1.97	17.9	1.10	5.24	32.0
1.50	1.97	17.9	1.10	5.46	42.0
1.50	1.97	17.9	1.10	5.62	53.0
1.50	1.97	17.9	1.10	5.77	66.0
1.50	1.81	18.2	1.00	4.63	16.0
1.50	1.81	18.2	1.00	4.73	23.0
1.50	1.81	18.2	1.00	4.93	31.0
1.50	1.81	18.2	1.00	4.99	40.0
1.50	1.81	18.2	1.00	5.34	56.0
1.50	1.81	18.2	1.00	5.60	66.0
1.50	1.81	20.6	0.937	4.74	12.0
1.50	1.81	20.6	0.937	4.84	17.0
1.50	1.81	20.6	0.937	5.15	23.0
1.50	1.81	20.6	0.937	5.21	30.0
1.50	1.81	20.6	0.937	5.44	41.0
1.50	1.81	20.6	0.937	5.55	50.0
1.50	1.81	20.6	0.937	5.72	58.0
1.50	1.81	20.6	0.937	5.86	66.0
1.50	1.97	21.8	0.977	5.10	15.0
1.50	1.97	21.8	0.977	5.35	18.0
1.50	1.97	21.8	0.977	5.64	23.0
1.50	1.97	21.8	0.977	5.87	33.0
1.50	1.97	21.8	0.977	5.97	47.0
1.50	1.97	21.8	0.977	6.15	57.0
1.50	1.97	21.8	0.977	6.36	66.0

Step height, *h* (cm)	**Discharge, Q (l/s)**	**y_0 (cm)**	**y_1 (cm)**	**y_3 (cm)**	**X (cm)**
1.50	1.64	21.6	0.826	4.17	10.0
1.50	1.64	21.6	0.826	4.31	14.0
1.50	1.64	21.6	0.826	4.55	18.0
1.50	1.64	21.6	0.826	4.68	21.0
1.50	1.64	21.6	0.826	4.89	26.0
1.50	1.64	21.6	0.826	5.14	46.0
1.50	1.64	21.6	0.826	5.34	55.0
1.50	1.64	21.6	0.826	5.40	66.0
2.00	4.42	20.0	2.42	8.16	35.0
2.00	4.42	20.0	2.42	8.33	53.0
2.00	4.42	20.0	2.42	8.57	60.0
2.00	4.42	20.0	2.42	8.74	66.0
2.00	3.64	20.2	1.92	7.08	20.0
2.00	3.64	20.2	1.92	7.15	30.0
2.00	3.64	20.2	1.92	7.46	46.0
2.00	3.64	20.2	1.92	7.59	54.0
2.00	3.64	20.2	1.92	7.79	66.0
2.00	3.19	20.9	1.66	6.69	20.0
2.00	3.19	20.9	1.66	6.98	30.0
2.00	3.19	20.9	1.66	7.17	39.0
2.00	3.19	20.9	1.66	7.25	45.0
2.00	3.19	20.9	1.66	7.40	51.0
2.00	3.19	20.9	1.66	7.61	60.0
2.00	3.19	20.9	1.66	7.70	66.0
2.00	2.86	21.0	1.48	6.00	15.0
2.00	2.86	21.0	1.48	6.26	24.0
2.00	2.86	21.0	1.48	6.42	33.0
2.00	2.86	21.0	1.48	6.62	44.0
2.00	2.86	21.0	1.48	6.83	53.0
2.00	2.86	21.0	1.48	7.05	66.0
2.00	3.19	23.8	1.53	6.83	19.0
2.00	3.19	23.8	1.53	6.97	22.0
2.00	3.19	23.8	1.53	7.27	33.0
2.00	3.19	23.8	1.53	7.47	46.0
2.00	3.19	23.8	1.53	7.77	52.0
2.00	3.19	23.8	1.53	7.96	66.0
2.00	2.86	24.1	1.37	6.31	15.0
2.00	2.86	24.1	1.37	6.69	22.0

Step height, *h* (cm)	**Discharge, Q (l/s)**	**y_0 (cm)**	**y_1 (cm)**	**y_3 (cm)**	**X (cm)**
2.00	2.86	24.1	1.37	6.86	33.0
2.00	2.86	24.1	1.37	7.13	42.0
2.00	2.86	24.1	1.37	7.25	48.0
2.00	2.86	24.1	1.37	7.33	59.0
2.00	2.86	24.1	1.37	7.57	66.0
2.00	2.53	23.7	1.21	5.51	16.0
2.00	2.53	23.7	1.21	5.69	20.0
2.00	2.53	23.7	1.21	5.87	25.0
2.00	2.53	23.7	1.21	6.11	32.0
2.00	2.53	23.7	1.21	6.44	40.0
2.00	2.53	23.7	1.21	6.69	53.0
2.00	2.53	23.7	1.21	6.98	66.0
2.00	2.42	23.7	1.15	5.34	15.0
2.00	2.42	23.7	1.15	5.59	19.0
2.00	2.42	23.7	1.15	5.73	23.0
2.00	2.42	23.7	1.15	5.98	23.0
2.00	2.42	23.7	1.15	6.27	38.0
2.00	2.42	23.7	1.15	6.48	46.0
2.00	2.42	23.7	1.15	6.68	55.0
2.00	2.42	23.7	1.15	6.92	66.0
2.50	5.14	22.7	2.69	8.23	40.0
2.50	5.14	22.7	2.69	8.72	49.0
2.50	5.14	22.7	2.69	9.07	55.0
2.50	5.14	22.7	2.69	9.30	58.0
2.50	5.14	22.7	2.69	9.45	66.0
2.50	4.61	23.7	2.35	8.11	29.0
2.50	4.61	23.7	2.35	8.34	35.0
2.50	4.61	23.7	2.35	8.52	40.0
2.50	4.61	23.7	2.35	8.71	48.0
2.50	4.61	23.7	2.35	8.83	58.0
2.50	4.61	23.7	2.35	8.93	66.0
2.50	4.25	24.5	2.09	7.55	22.0
2.50	4.25	24.5	2.09	7.66	27.0
2.50	4.25	24.5	2.09	7.84	30.0
2.50	4.25	24.5	2.09	8.07	38.0
2.50	4.25	24.5	2.09	8.22	42.0
2.50	4.25	24.5	2.09	8.54	47.0
2.50	4.25	24.5	2.09	8.77	55.0

Step height, *h* (cm)	**Discharge, Q (l/s)**	**y_0 (cm)**	**y_1 (cm)**	**y_3 (cm)**	***X* (cm)**
2.50	4.25	24.5	2.09	9.03	66.0
2.50	3.78	24.5	1.82	7.28	19.0
2.50	3.78	24.5	1.82	7.47	24.0
2.50	3.78	24.5	1.82	7.52	28.0
2.50	3.78	24.5	1.82	7.60	33.0
2.50	3.78	24.5	1.82	7.77	38.0
2.50	3.78	24.5	1.82	7.83	42.0
2.50	3.78	24.5	1.82	8.14	54.0
2.50	3.78	24.5	1.82	8.35	66.0
2.50	3.78	24.7	1.79	7.26	22.0
2.50	3.78	24.7	1.79	7.49	29.0
2.50	3.78	24.7	1.79	7.84	40.0
2.50	3.78	24.7	1.79	8.07	48.0
2.50	3.78	24.7	1.79	8.19	51.0
2.50	3.78	24.7	1.79	8.39	57.0
2.50	3.78	24.7	1.79	8.52	66.0
2.50	3.61	24.9	1.72	6.69	21.0
2.50	3.61	24.9	1.72	7.06	26.0
2.50	3.61	24.9	1.72	7.23	33.0
2.50	3.61	24.9	1.72	7.36	40.0
2.50	3.61	24.9	1.72	7.53	44.0
2.50	3.61	24.9	1.72	7.83	54.0
2.50	3.61	24.9	1.72	7.99	59.0
2.50	3.61	24.9	1.72	8.20	66.0

Appendix B

Table B-1- Raw experimental data for the abrupt step sweep-out limit testing

Step height, *h* (cm)	**Discharge, Q (l/s)**	**y_0 (cm)**	**y_1 (cm)**	**y_3 (cm)**	***X* (cm)**
1.00	2.19	13.5	1.48	5.61	34.0
1.00	1.67	12.0	1.10	4.17	23.0
1.00	1.28	13.7	0.805	3.55	18.0
1.00	1.67	17.1	0.930	4.94	15.0
1.00	1.28	16.8	0.720	3.99	13.0
1.00	1.28	18.5	0.690	4.10	13.0
1.00	1.28	20.3	0.651	4.04	10.0
1.00	1.28	22.3	0.614	4.32	11.0
1.50	2.39	14.5	1.50	5.28	37.0
1.50	2.53	16.4	1.50	5.83	31.0
1.50	2.22	15.3	1.35	5.06	33.0
1.50	2.22	18.5	1.25	5.62	24.0
1.50	1.97	17.9	1.10	4.91	17.0
1.50	1.81	18.2	1.00	4.63	16.0
1.50	1.81	20.6	0.937	4.74	12.0
1.50	1.97	21.8	0.977	5.10	15.0
1.50	1.64	21.6	0.826	4.17	10.0
2.00	4.42	20.0	2.42	8.16	35.0
2.00	3.64	20.2	1.92	7.08	20.0
2.00	3.19	20.9	1.66	6.69	20.0
2.00	2.86	21.0	1.48	6.00	15.0
2.00	3.19	23.8	1.53	6.83	19.0
2.00	2.86	24.1	1.37	6.31	15.0
2.00	2.53	23.7	1.21	5.51	16.0
2.00	2.42	23.7	1.15	5.34	15.0
2.50	5.14	22.7	2.69	8.23	40.0
2.50	4.61	23.7	2.35	8.11	29.0
2.50	4.25	24.5	2.09	7.55	22.0
2.50	3.78	24.5	1.82	7.28	19.0
2.50	3.78	24.7	1.79	7.26	22.0
2.50	3.61	24.9	1.72	6.69	21.0

Appendix C

Table C-1- Raw experimental data for the lower boundary hysteresis testing

Step slope	**Discharge, Q (l/s)**	y_0 **(cm)**	y_1 **(cm)**	y_3 **(cm)**	X **(cm)**
Abrupt	2.19	13.3	1.48	5.62	41.0
Abrupt	1.67	13.3	1.10	4.60	25.0
Abrupt	1.28	13.8	0.805	3.79	13.0
Abrupt	1.28	16.9	0.720	4.02	11.0
Abrupt	1.28	21.5	0.651	4.18	7.0
1-in-1	1.28	13.9	0.809	4.36	58.0
1-in-1	1.00	19.7	0.529	3.98	38.0
1-in-1	1.00	15.7	0.589	3.70	42.0
1-in-1	1.00	13.5	0.640	3.46	45.0
1-in-1	0.861	16.3	0.499	3.29	37.0
1-in-1	0.861	13.2	0.550	2.97	44.0
1-in-2	0.917	19.7	0.466	3.88	43.0
1-in-2	0.917	17.2	0.499	3.77	50.0
1-in-2	0.917	15.0	0.550	3.59	55.0
1-in-2	1.11	13.7	0.700	4.01	62.0
1-in-2	1.25	13.4	0.800	4.35	63.0
1-in-2	1.47	11.6	1.02	4.48	61.0
1-in-2	1.03	15.9	0.600	4.02	57.0
1-in-2	1.03	13.9	0.640	3.90	57.0
1-in-2	0.917	12.2	0.600	3.21	58.0
1-in-3	0.889	18.5	0.490	3.87	54.0
1-in-3	0.889	14.5	0.540	3.67	61.0
1-in-3	0.889	12.3	0.579	3.41	64.0
1-in-3	0.694	17.0	0.399	3.22	58.0
1-in-4	0.889	16.8	0.499	3.83	59.0
1-in-4	0.722	20.9	0.350	3.48	53.0
1-in-4	0.778	16.9	0.438	3.50	60.0
1-in-4	0.778	19.4	0.409	3.59	54.0

Appendix D

Table D-1- Raw experimental data for the upper boundary hysteresis testing

Step slope	Discharge, Q (l/s)	y_0 (cm)	y_1 (cm)	y_3 (cm)	X (cm)
Abrupt	2.19	13.3	1.48	5.45	19.0
Abrupt	1.67	13.3	1.10	4.51	10.0
Abrupt	1.28	13.8	0.805	3.64	7.0
Abrupt	1.28	16.9	0.720	3.95	10.0
Abrupt	1.28	21.5	0.651	4.13	7.0
1-in-1	1.28	13.9	0.809	3.76	23.0
1-in-1	1.00	19.7	0.529	3.44	10.0
1-in-1	1.00	15.7	0.589	3.33	20.0
1-in-1	1.00	13.5	0.640	3.16	20.0
1-in-1	1.58	11.9	1.10	4.16	32.0
1-in-1	1.33	11.7	0.921	3.38	22.0
1-in-1	0.861	16.3	0.499	3.07	24.0
1-in-2	0.917	19.7	0.466	3.48	20.0
1-in-2	0.917	17.2	0.499	3.30	25.0
1-in-2	0.917	15.0	0.550	3.03	20.0
1-in-2	1.11	13.7	0.700	3.49	23.0
1-in-2	1.25	13.4	0.800	3.75	26.0
1-in-2	1.47	11.6	1.02	4.00	31.0
1-in-2	1.03	15.9	0.600	3.48	25.0
1-in-2	1.03	13.9	0.640	3.30	23.0
1-in-3	0.889	18.5	0.490	3.43	29.0
1-in-3	0.889	14.5	0.540	2.99	27.0
1-in-3	0.889	12.3	0.579	2.70	28.0
1-in-3	1.03	13.9	0.627	3.33	24.0
1-in-3	0.694	17.0	0.399	2.77	37.0
1-in-3	1.11	12.1	0.750	3.26	24.0
1-in-3	1.17	12.2	0.790	3.50	31.0
1-in-4	0.889	16.8	0.499	3.08	22.0
1-in-4	0.889	15.3	0.530	3.07	26.0
1-in-4	1.00	14.0	0.620	3.27	30.0
1-in-4	0.722	20.9	0.350	2.86	27.0
1-in-4	0.778	16.9	0.438	2.81	28.0
1-in-4	0.778	19.4	0.409	3.09	30.0
1-in-4	1.03	12.0	0.700	2.89	25.0
1-in-4	0.944	14.8	0.570	3.03	24.0